Two phases of Mesozoic north-south extension in the eastern Altyn Tagh range, northern Tibetan Plateau

Xuanhua Chen,[1] An Yin,[2] George E. Gehrels,[3] Eric S. Cowgill,[2] Marty Grove,[2] T. Mark Harrison,[2] and Xiao-Feng Wang[1]

[1]   The >300-km long, east striking Lapeiquan fault lies in the eastern Altyn Tagh range along the northern margin of the Tibetan Plateau and was interpreted as a north dipping thrust in early studies. However, our mapping shows that the fault is a south dipping normal fault juxtaposing Archean-Proterozoic gneisses beneath an early Paleozoic volcanic and sedimentary sequence. Its dip angle varies from <30° to ~60°. The central fault segment is expressed as a 30–50 m thick ductile shear zone with well-developed mylonitic fabrics and stretching mineral lineations, where the eastern and western segments are characterized by cataclastic deformation. Kinematic indicators such as asymmetric boudinage, asymmetric folds, and minor brittle and ductile faults within the fault zone consistently indicate a top-south normal-slip sense of shear. The age of the Lapeiquan fault is constrained by two types of information. First, a sequence of Early-Middle Jurassic sediments is locally present in the hanging wall of the Lapeiquan fault. The clasts of the Jurassic strata, particularly the stromatolite-bearing, cherty limestone and purple quartzite, can be correlated uniquely with those in the footwall of the fault. We interpret that the Early-Middle Jurassic strata were deposited in an extensional basin related to motion along the Lapeiquan fault. Second, $^{40}Ar/^{39}Ar$ thermochronologic analyses indicate two prominent cooling events in the Lapeiquan footwall. The older event occurred in the latest Triassic-earliest Jurassic between ~220 and 187 Ma, while the younger event occurred in the latest Early Cretaceous at ~100 Ma. Because the 220–187 Ma cooling ages are widespread in the Lapeiquan footwall, we suggest it to represent the main stage of faulting. We interpreted the younger phase of fault motion at ~100 Ma to have been related to fault reactivation. The deformation was aided by motion along the south dipping Qiashikan normal fault that merges with the eastern Lapeiqaun fault. From the regional tectonic setting, it appears that Mesozoic extension in northern Tibet to have occurred in a back arc setting during northward subduction of the Tethyan oceanic plate. The findings of Mesozoic extensional structures in northern Tibet suggest that compressive stress induced by collision of the Qiangtang and Lhasa terranes with Asia was not transmitted beyond northern Tibet. This in turn implies that the popularly inferred contractional setting for Mesozoic evolution of the Tian Shan north of Tibet needs a reevaluation based on a combination of both structural and sedimentological observations.   *INDEX TERMS*: 8157 Tectonophysics: Plate motions—past (3040); 8199 Tectonophysics: General or miscellaneous; 9320 Information Related to Geographic Region: Asia; *KEYWORDS*: Tibetan Plateau, Altyn Tagh fault, extensional tectonics. **Citation:** Chen, X., A. Yin, G. E. Gehrels, E. S. Cowgill, M. Grove, T. M. Harrison, and X.-F. Wang, Two phases of Mesozoic north-south extension in the eastern Altyn Tagh range, northern Tibetan Plateau, *Tectonics*, *22*(5), 1053, doi:10.1029/2001TC001336, 2003.

1. Introduction

[2]   One of the major challenges in determining the role of the Indo-Asian collision in creating the Tibetan Plateau is to remove the effect of widespread Paleozoic and Mesozoic deformation in the region [e.g., *Yin and Nie*, 1996; *Murphy et al.*, 1997]. Because the Paleozoic and Mesozoic geologic history of the Tibetan Plateau remains poorly defined, our ability in determining the mechanism under which the Tibetan Plateau has developed in the Cenozoic has been severely hampered. The Phanerozoic tectonic evolution of the Tibetan region was traditionally viewed as having been dominated by contractional deformation resulted from successive accretion of micro-continents and arc terranes onto the southern margin of Asia [*Chang and Zheng*, 1973; *Allègre et al.*, 1984; *Dewey et al.*, 1988]. These collisional events along the southern margin of Asia were thought to have affected the basin development in the Tarim and Tian Shan areas, creating large intracontinental thrust-related basins [e.g., *Hendrix et al.*, 1992; *Ritts and Biffi*, 2000]. However, recent discoveries of Mesozoic detachment faults in Tibet [*Kapp et al.*, 2000], Mongolia [*Zheng and Zhang*, 1994; *Webb et al.*, 1999], and north China [*Darby et al.*, 2001; *Davis et al.*, 2001a, 2001b; *Ratschbacher et al.*, 2000] highlight the importance of extension in shaping the geologic framework of east Asia.

---

[1]Institute of Geomechanics, Chinese Academy of Geological Sciences, Beijing, China.
[2]Department of Earth and Space Sciences, University of California, Los Angeles, California, USA.
[3]Department of Geosciences, University of Arizona, Tucson, Arizona, USA.

[3] As shown by *Kong et al.* [1997], pre-Cenozoic tectonic history may have played a decisive role in controlling the kinematics and dynamics of Tibetan Plateau formation during the Indo-Asian collision. First, the pre-existing sutures are loci of north-south contraction and large-scale strike-slip faults. Second, the velocity field of the collision zone (i.e., north-south shortening versus eastward extrusion) is very sensitive to gravitational force as represented by pre-existing topography. From the geologic point of view, Mesozoic extension in central Tibet has played a key role in localizing Cenozoic crustal shortening and magmatism during the Indo-Asian collision [*Yin and Harrison*, 2000].

[4] In this paper, we report the discovery of major Mesozoic extensional fault systems in the eastern Altyn Tagh range along the northern margin of the Tibetan Plateau (Figure 1). Based on newly obtained U-Pb zircon and ^{40}Ar/^{39}Ar thermochronologic data, field relationship established by our mapping, and correlation of regional geology, we suggest that extensional faulting in the eastern Altyn Tagh region occurred in two phases, one during the Early Jurassic and another during the late Early Cretaceous. Our timing of extensional events in northern Tibet correlates remarkably well with those in north China described by *Darby et al.* [2001] and *Davis et al.* [2001a, 2001b], implying regional importance of Mesozoic episodic extensional tectonics in China.

2. Geology of the Altyn Tagh Range

[5] The Altyn Tagh range separates the Tarim basin in the north from the Tibetan Plateau in the south (Figure 1). Within the context of the Late Cenozoic regional tectonic framework, the Altyn Tagh massif lies entirely north of the active left-slip Altyn Tagh fault [*Burchfiel et al.*, 1989].

[6] The geology of the Altyn Tagh range east of the Mangnai-Rouqiang Road is better known than that in the western Altyn Tagh. East of the road, unpublished Chinese geologic maps at a scale of 1:200,000 are available, whereas the most detailed geologic maps for the western Altyn Tagh region are at a scale of 1:1,000,000. Lithologically, the Altyn Tagh range consists of Archean and Proterozoic metamorphic gneisses along its northeastern edge [*Xinjiang Bureau of Geology and Mineral Resources (BGMR)*, 1993; *Che et al.*, 1995a] (Figures 1 and 2). Proterozoic stromatolite-bearing sedimentary sequences, consisting mostly of thickly bedded quartzite and cherty limestone, are present in the central and eastern range [*Xinjiang BGMR*, 1993; this study]. Early Paleozoic volcanic and marine sediments are exclusively exposed in the eastern Altyn Tagh range, whereas Precambrian marble, schist, and quartzo-feldspathic gneisses dominate in the western Altyn Tagh range [*Xinjiang BGMR*, 1993]. The apparent absence of early Paleozoic rocks in the western Altyn Tagh range as shown in regional geologic maps [*Liu*, 1988; *Xinjiang BGMR*, 1993] is most likely a result of lack of detailed geologic studies. Devonian strata are typically siliciclastic sediments, whereas Carboniferous rocks are shallow marine sediments [*Xinjiang BGMR*, 1993]. Coal-bearing Jurassic continental sediments are also scattered throughout the region, whereas Cretaceous strata are only exposed in the southwestern edge of the range east of Qiemo [*Xinjiang BGMR*, 1993; also see *Cowgill et al.*, 2000].

[7] In the eastern Altyn Tagh range, Cenozoic deformation is expressed primarily by several east striking Tertiary thrusts that bound Late Eocene-Early Oligocene basins (Figure 2). These structures and basins are truncated by the Altyn Tagh fault [*Yin and Harrison*, 2000]. In the western portion of the range, its northern margin is defined by the east-northeast striking, left-slip Jianglisai fault, which may have been kinematically linked with the east striking Tertiary thrusts in the eastern Altyn Tagh massif [*Cowgill et al.*, 2000; *Yin and Harrison*, 2000]. *Cowgill et al.* [2000] suggest that coeval Cenozoic motion along the Altyn Tagh fault, the Jianglisai fault, and thrusts in the eastern Altyn Tagh range may define a large-scale strike-slip duplex system.

Figure 1. (opposite) (a) Tectonic map of eastern Asia (modified after *Yin and Nie* [1996]) and locations of major Jurassic-Cretaceous extensional systems: DB, northern Dabie core complex [*Ratschbacher et al.*, 2000]; DQ, Daqing Shan extensional fault system [*Darby et al.*, 2001], GC, Gangma Co detachment fault [*Kapp et al.*, 2000], HCC, Huhhot core complex [*Zheng et al.*, 2001]; JQ, Jiuquan extensional system [*Huo and Tan*, 1995]; L, Liaonan detachment system [*Yin and Nie*, 1996]; LS, Lu Shan core complex [*Lin et al.*, 2000]; MC. Minle and Chaoshui extensional Basins [*Vincent and Allen*, 1999]; SH, Shuanghu detachment fault system [*Kapp et al.*, 2000]; YM, Yunmeng Shan core complex [*Davis et al.*, 1996]; YG, Yagong core complex [*Zheng and Zhang*, 1994; *Webb et al.*, 1999]. Major sutures are also shown: IYS, Indus-Yalu suture; BNS, Bangong-Nujiang suture; JS, Jinsha suture; KS, Kunlun suture; SQS, southern Qilian suture; NQS, northern Qilian suture; TYS, northern Tian Shan and Yin Shan suture; NTS, northern Tian Shan suture. (b) Simplified geologic map of the eastern Altyn Tagh Range and Qilian Shan. Major geologic terranes are as follows. Ar/Pt, late Archean to early Proterozoic crystalline basement rocks. QTS, Quantan Shan terrane (mainly Precambrian crystalline rocks, but also consisting of early Paleozoic volcanic and marine sedimentary sequence and Jurassic sedimentary strata). NQ, northern Qilian terrane (volcanic arc sequence and subduction melange, intruded by early Paleozoic plutons). CQ, central Qilian terrane (Proterozoic passive continental sequence, interpreted to be the cover sequence of North China crystalline basement rocks). YM, Yiema Nan Shan terrane (mostly flysch complex and locally melange complex consisting of ultramafic fragments, intruded by early Paleozoic plutons). DH, Danghe Nan Shan terrane, mostly pillow basalts interlayered locally with graywackes). DJ, Dajin Shan terrane (dominantly ductilely folded and metamorphosed graywacke sequences with the presence of biotite and chlorites). NQD, north Qaidam metamorphic belt (mostly biotite ± garnet quartzo-feldsparthic gneiss). KLA, Kunlun arc terrane, consisting mostly of Ordovician and Permian-Triassic plutonic and volcanic rocks. Major structures: ATF, Altyn Tagh fault; JW suture, Jianglisai-Washixia suture.

[8] Two east trending early Paleozoic suture zones have been proposed in the Altyn Tagh range: the Hongliugou suture in the east and Jianglisai-Washixia suture in the west [e.g., *Che et al.*, 1995a, 1995b; *Liu et al.*, 1997, 1999; *Sobel and Arnoad*, 1999; *Yin and Harrison*, 2000; *Zhang et al.*, 2001]. The suture zones typically consist of sparse ultramafic fragments and are laterally discontinuous. They

are highly modified by the subsequent Mesozoic and Cenozoic deformation. Noticeably, ultramafic fragments are distributed along the Altyn Tagh fault and on both sides of the Lapeiquan fault to be described below. As a result of these complexities, the extent and original orientations of the suture zones remain poorly defined. Along the Hongliugou suture zone, several small ultramafic bod-

(A)

(B)
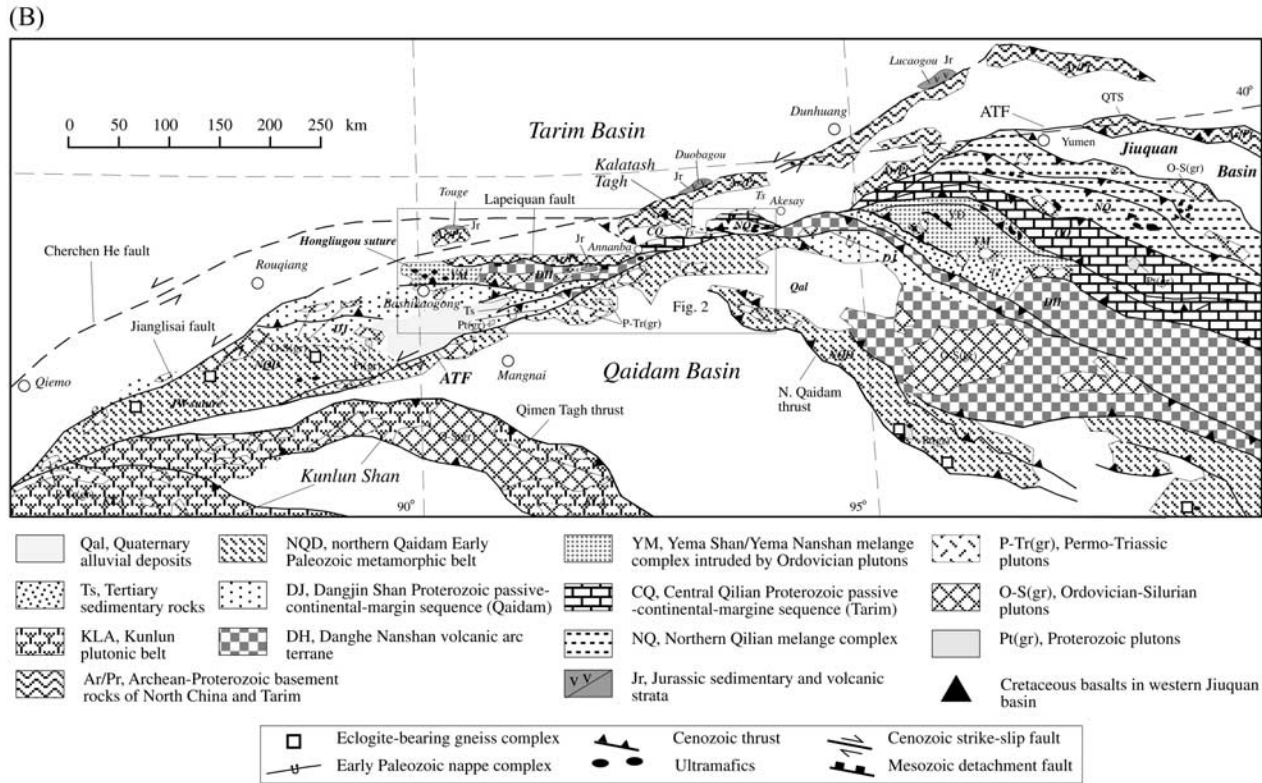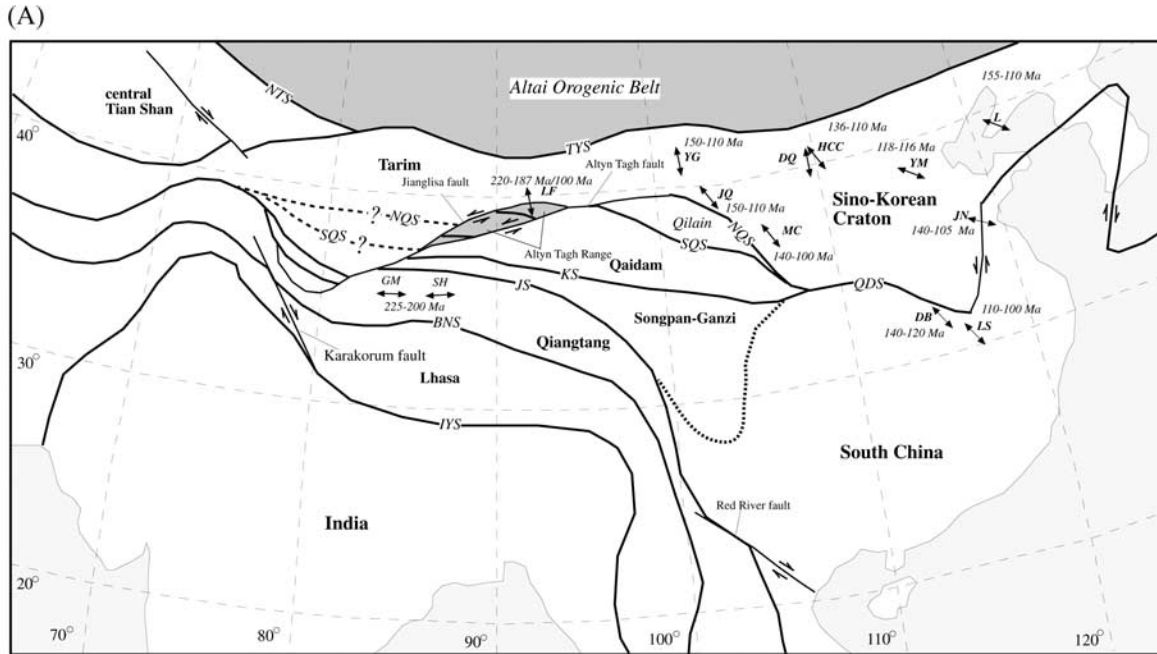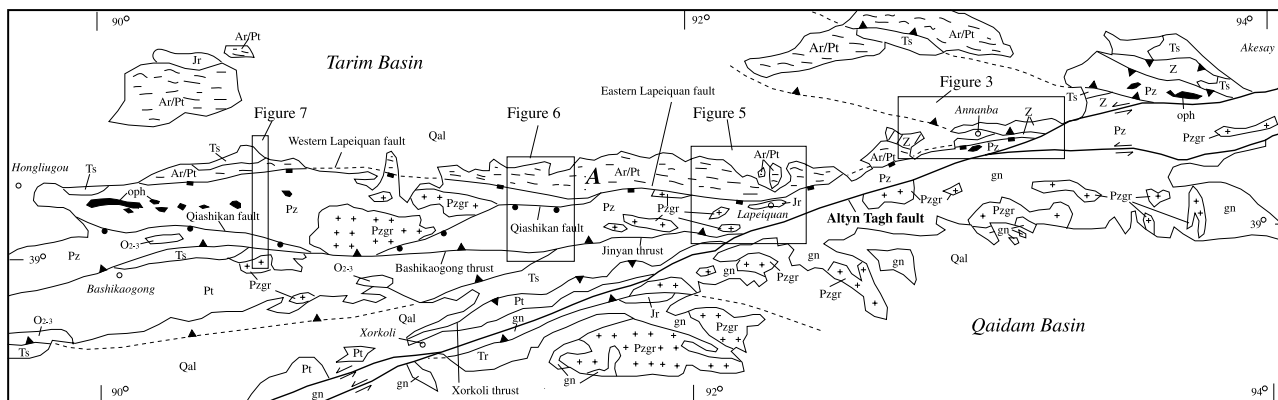
Figure 2. Simplified geologic map of eastern Altyn Tagh range based on *Liu* [1988], *Xinjiang BGMR* [1981a, 1981b, 1981c, and 1981d], analysis of Landsat images, and our own field observations. Locations of Figures 3, 5, 6, and 7 are also shown. Those areas were studied in detail by this study. Symbols in the map: Qal, Quaternary alluvial deposits; Ts, Tertiary red beds, mostly late Eocene to early Oligocene sediments [*Xinjiang BGMR*, 1981c, 1981d]; Jr, Jurassic strata; Tr, Triassic strata; Pz, early Paleozoic volcanic and marine sedimentary rocks, most likely Ordovician and Silurian in age [*Xinjiang BGMR*, 1981c, 1981d]; O2-3, Middle and Late Ordovician limestone and graywacke; Pzgr, early Paleozoic granitoids; Z, Late Proterozoic shallow marine quartzite and cherty limestone in the footwall of the Lapeiquan fault [*Xinjiang BGMR*, 1981a, 1981b], Pt, Proterozoic stramatolite-bearing limestone, marbles, schist, and quartzite in the hanging wall of the Lapeiquan fault; gn, quartzo-feldsparthic gneiss south of the Altyn Tagh fault; Ar/Pt, Archean-Proterozoic gneiss in the footwall of the lapeiquan fault, most likely represent the basement of the Tarim basin. Note that the east striking Tertiary Xorkoli and Jinyan thrusts and the Lapeiquan fault are all truncated by the east-northeast striking Altyn Tagh fault. Also note that the Qiashikan fault is cut by the Jinyan-Bashikaogong thrust system but merges with the Lapeiquan fault. The intersection point of the two faults (point A) partitions the Lapeiquan fault into the western and eastern segments. The eastern segment was reactivated in the latest Early Cretaceous and was kinematically linked with the coeval Qiashikan fault.

ies are exposed near Bashikaogong, Annanba, and Akesay (Figure 2) [*Xingjing BGMR*, 1981a; *Liu*, 1988; *Xinjiang BGMR*, 1993]. In Hongliugou, the ultramafic rocks are exposed as tectonic slices juxtaposed by faults against high-grade gneiss ($T = 550° ± 30°C$, $P = 1.4-2.0$ GPa), pillow basalts, chert, marble, flysch, and locally volcaniclastic conglomerates [*Xinjiang BGMR*, 1981a; *Che et al.*, 1995b; *Liu et al.*, 1999; this study]. The suture zone rocks are located in the hanging wall of the south dipping Lapeiquan fault. The pillow basalts and flysch are intruded by early Paleozoic plutons (Figure 2) [*Xinjiang BGMR*, 1981a]. Ultramafic rocks and deep marine flysch sediments are also exposed at the eastern tip of the Altyn Tagh range near Akesay. These rocks are shown on the south side of the Altyn Tagh fault on regional geologic maps [e.g., *Liu*, 1988]. However, our field observation shows that the Akesay ultramafic rocks are located north of the Altyn Tagh fault and in the footwall of the south dipping Lapeiquan fault. The ultramafic rocks together with a complexly folded flysch sequence are thrust over the Proterozoic shelf sequence of the Tarim block. The latter in turn is thrust over Tertiary sediments (Figure 1). The Akesay ultramafic complex represents the easternmost end of the Hongliugou suture, which is truncated by the Altyn Tagh fault. The Hongliugou suture is complexly deformed by Mesozoic and Cenozoic faults and its exposure is very limited. As a result, exactly what tectonic plates (i.e., North China, Tarim, Qaidam, or Qilian terranes) it separates, the polarity of subduction, and how it extends westward remain poorly constrained (see discussion by *Sobel and Arnoad* [1999] [cf. *Yin and Nie*, 1996]).

[9] Muscovites from the high-grade gneiss in the Hongliugou suture zone near Bashikaogong yielded $^{40}Ar/^{39}Ar$ cooling ages of $575 ± 3$ Ma and $573 ± 6$ Ma, which are interpreted to represent an exhumation event during subduction beneath and accretional tectonics along the southern margin of the Tarim block [*Che et al.*, 1995a]. *Yang et al.* [2001] placed the age of ocean closure along the Hongliugou suture to be early Paleozoic based on its possible correlation with the northern Qilian suture zone south of the Altyn Tagh fault. *Sobel and Arnoad* [1999] reported Late Ordovician-Early Silurian $^{40}Ar/^{39}Ar$ cooling ages of muscovite and biotite from schists, gneiss, and deformed granodiorite along the Mangnai-Rouqiang road in the central Altyn Tagh and along a traverse across the eastern Altyn Tagh range near Lapeiquan (Figure 1). They suggest the cooling event to have been induced by collision and underthrusting of the Tarim block in the north below a continental arc in the south. Their interpretation is in many respects similar to earlier suggestion of *Che et al.* [1995a, 1995b]. However, because Ordovician and Silurian plutons are common in both traverses where *Sobel and Arnoad*'s [1999] samples were collected [*Cowgill*, 2001; *Gehrels et al.*, 2003], the cooling ages reported by *Sobel and Arnoad*

[1999] most likely reflect the time of plutonic emplacement instead of a collisional event as envisaged by these authors. As will be discussed below, the cooling history of the eastern Altyn Tagh range is complex. In addition to Ordovician-Silurian cooling events, Jurassic and Cretaceous cooling ages of muscovite, biotite, and K-feldspar are also common. Their geologic significance has just begun to be understood in light of a structural framework established by this study.

[10] Because the Altyn Tagh fault offsets the Paleozoic Kunlun batholith belt for ~500 km [e.g., *Peltzer and Tapponnier*, 1988; *Cowgill*, 2001], *Yin and Nie* [1996] proposed the Qilian suture to have been offset to the central Altyn Tagh range that separates Tarim into the northern and southern blocks. This proposal appears to be at odds with the observation that Ordovician marine strata are continuous across the projected suture [*Jia*, 1997]. To resolve this problem, *Guo et al.* [2001] suggest instead that ocean closure in central Tarim occurred in the late Proterozoic. This is based on Sm-Nd dating of gabbro and basalt from the Hongliugou suture zone that yields an isochron age of 829 ± 60 Ma for a gabbro sample and an age of 949 ± 62 Ma for a mix of gabbro and basalt. We believe that these ages only present the age of the oceanic crust consumed by the suture and should not be interpreted as indicating the time of suturing. Therefore, where is the Qilian suture zone north of the Altyn Tagh fault and how it extends into the Tarim basin and beyond to the west remain unresolved.

[11] Another inferred suture zone in the Altyn Tagh range is the Jianglisai-Washixia belt (Figure 1), which is marked by the presence of ultramafic fragments and eclogite-bearing high-grade gneiss complexes [*Liu et al.*, 1997]. The conditions for the formation of the eclogite are $P = 1.40-1.85$ GPa and $T = 660°-830°C$ as estimated *by Liu et al.* [1997] and $P = 1.1-1.4$ GPa and $T = 670°-800°C$ as estimated by *Zhang et al.* [2001], respectively. The Sm-Nd isotopic data from the eclogite in the inferred suture yield a whole rock-garnet-omphacite isochron of 500 ± 10 Ma, and U-Pb zircon ages of 504 ± 5 Ma [*Zhang et al.*, 2001]. These ages were interpreted by the above authors to represent the age of suturing in the western Altyn Tagh. Similar to the problem of the Hongliugou suture, how the Jianglisai-Washixia suture extends westward beneath the Cenozoic Tarim basin is unclear.

3. Geology of the Lapeiquan Normal Fault System

[12] A prominent fault that separates Archean-Proterozoic gneiss (Unit Ar/Pt in Figure 2) and a late Proterozoic shallow-marine sequence (Unit Z in Figure 2) from Paleozoic volcanic and sedimentary rocks (Unit Pz in Figure 2) is exposed along the northern margin of the Tibetan Plateau in the eastern Altyn Tagh range [*Liu*, 1988; *Xinjiang BGMR*, 1993]. This fault, referred to as the Lapeiquan fault by the *Chinese State Bureau of Seismology* (CSBS) [1992], extends for about 300 km from Hongliugou (~90°E) in the west to Annanba (~93°E) in the east (Figure 1). The Lapeiquan fault is truncated by the Altyn Tagh fault in the east and

extends beneath Quaternary sediments of the Tarim basin in the west (Figure 2). In the existing 1:200,000 geologic maps [*Xinjiang BGMR*, 1981a, 1981b, 1981c, 1981d, 1986], the Lapeiquan fault has been consistently shown as a north dipping thrust, putting the Archean-Proterozoic gneisses of the Tarim basement [*Che and Sun*, 1996] over the Paleozoic volcanic and sedimentary strata [*Liu*, 1988]. However, our geologic mapping and structural observations across this fault indicate that the fault is south dipping and normal-slip. In the following sections, we describe the characteristics of this fault system along four traverses.

3.1. Annanba Area

[13] The Lapeiquan fault in this area is well exposed south of Annanba and dips $30°-40°$ to the south. Its fault zone is best exposed along a river cut south of Annanba. It consists of $30-50$ m thick zone of fine-grained fault gouge and cm-scale highly sheared blocks of siltstone, metavolcanic rocks, and limestone. The volcanic rocks in the hanging wall are locally juxtaposed with ultramafic fragments that may be part of the Hongliugou suture zone [*Xinjiang BGMR*, 1981b, 1981c]. Bedding in the sheared rock fragments in the fault zone is variably discordant with shear surfaces due to fracturing and rotation. At one location the sense of rotated clasts in the fault zone indicates a down-to-the-south sense of motion. Due to extensive development of fine-grained fault gorge, striations are poorly development. As a result, we were not able to carry out a detailed kinematic study of the fault zone at this location. On map view, the eastern end of the east striking Lapeiquan fault is truncated by the active north-northeast striking left-slip Altyn Tagh fault and may have been offset for more than 250 km [*Yin et al.*, 2000].

[14] The age of the hanging wall sequence was first assigned as late Proterozoic [*Xinjiang BGMR*, 1981b], although neither fossils nor radiometric ages were provided. The same lithologic sequence near Lapeiquan along strike immediately to the west of the Annanba area was assigned to be Late Ordovician as indicated by the presence of marine fossils [*Xinjiang BGMR*, 1981d]. Based on this information, we interpret the age of the rocks directly above the Lapeiquan fault to be early Paleozoic.

[15] The footwall rocks of the Lapeiquan fault in the Annanba area are a sequence of shallow marine quartzite and cherty limestone. The sequence dips gently to the north. Both ripple marks and cross-beddings are abundant in the purple quartzite layers, whereas limestone beds contain stromatolite and cm-scale cherty layers (Figure 4a). Highly altered mafic sills intruding cherty limestone were also observed in the field. The age of the footwall sequence has been assigned to be Late Proterozoic based on the presence of stromatolite [*Xinjiang BGMR*, 1981b]. To the west, the Annanba Late Proterozoic sedimentary sequence is unconformably on top of the Archean-Proterozoic gneisses (Figure 4b). This contact was originally mapped as a fault by *Xinjiang BGMR* [1981c]. The contact between the crystalline basement and Proterozoic sedimentary sequence is truncated by the Lapeiquan fault (Figure 3), indicating that the Lapeiquan fault cuts progressively deeper crustal section westward and its vertical stratigraphic throw
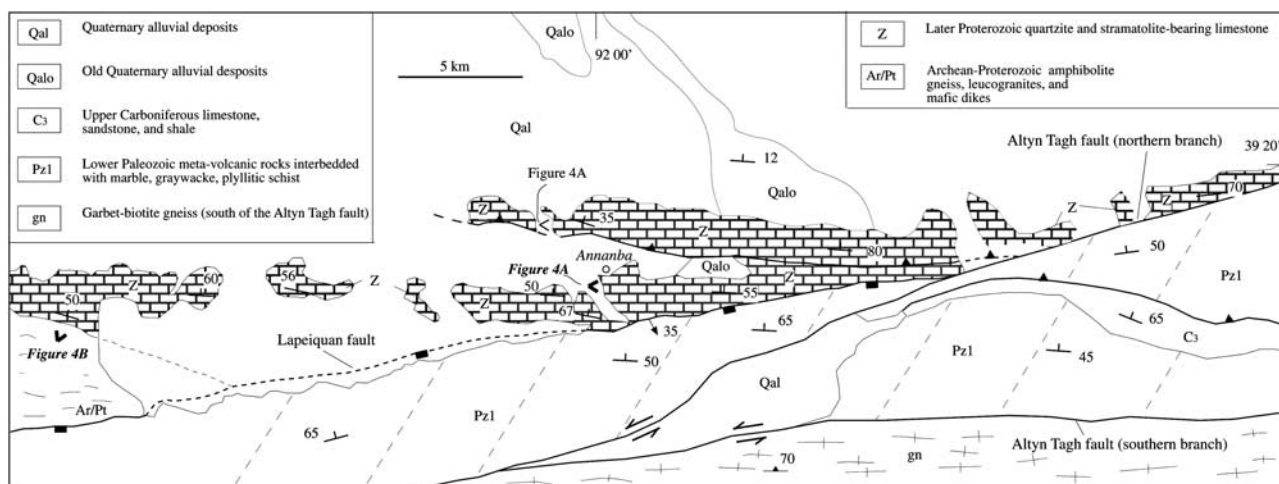
Figure 3. Simplified geologic map of the Annanba area based on our reconnaissance mapping, analysis of Landsat images, and reinterpretation of the existing geologic maps at a scale of 1:200,000 and 1:1.5 M [*Xinjiang BGMR*, 1981b, 1981c, 1986; *Liu*, 1988]. Note that the Lapeiquan fault cuts deeper crustal section westward. It is truncated in the east by the active Altyn Tagh fault.

decreases eastward (Figure 2). Although we did not perform detailed kinematic analysis of fault zone deformation, the younger-over-older field relationship and relatively low-angle dip of the fault zone are suggestive of normal sense motion along this segment of the Lapeiquan fault.

[16] An active north dipping thrust immediately north of Annanba repeats the Late Proterozoic stratigraphic section and tilted a Quaternary alluvial fan northward (Figure 3). The development of this thrust is related to the presence of a large restraining bend along the active Altyn Tagh fault system that produces two strands in this area (Figure 2). Both strands strike east and depart significantly from its regional strike of N65°E (Figure 2). Several minor thrusts with offset of <50 cm are observed in the limestone beds in the footwall of the active thrust.

3.2. Lapeiquan Area

[17] The south dipping Lapeiquan fault in this area juxtaposes early Paleozoic volcanic and sedimentary rocks, Carboniferous limestone and shale, and Lower and Middle Jurassic strata over Archean and Proterozoic gneisses (Figure 4). Our age assignment of the lithologic units follows that of *Xinjiang BGMR* [1981d, 1993] and *Che and Sun* [1996]. Footwall rocks of the fault consist of foliated diorite that were intruded first by K-feldspar rich granite followed by intrusion of west-northwest trending mafic dike swarms. The dikes are truncated in the east by the Lapeiquan fault. Foliation in the footwall gneisses is folded both at an outcrop scale as isoclinal folds (a few meters of wavelengths and amplitudes) and as broad east-plunging antiforms and synforms (5−6 km wavelength and 1−2 km amplitude) at a map scale (Figure 5).

[18] The Lapeiquan fault dips ∼30° to the south. Locally, its dip can be as low as ∼15°. Where exposed, the fault is expressed as a ∼2-m thick zone of yellow fault gouge. In

two places we observed striations on the fault surface, one trending to the south and plunge at 15° and another trending S30°W and plunge at 35°. The crystalline rocks below the Lapeiquan fault exhibit little brittle deformation. We observed no mylonite associated with the fault at this location. Immediately above the fault is the Upper Ordovician volcanic strata interbedded with limestone, shale, and graywacke [*Xinjiang BGMR*, 1981d] (Figure 5). Bedding of this unit directly above the fault defines numerous small-scale asymmetric folds (10−20 cm wavelength and 5−10 cm in amplitude), all verging to the south. In addition, mesoscopic-scale faults that are directly above and parallel to the Lapeiquan fault have offsets of a few centimeters to tens of centimeters and show consistent top-south normal slip (Figure 4c). We relate the development of small asymmetric folds and hanging wall minor normal faults to motion along the Lapeiquan fault. The correlation suggests that the fault is normal-slip.

[19] Structures south of the Lapeiquan fault are characterized by two oppositely dipping Tertiary thrusts: the north dipping Jinyan thrust in the and the south dipping Xorkoli thrust in the south (Figure 2). The contacts represented by the Jinyan and Xorkoli thrusts were originally mapped as unconformities between Tertiary strata above and Precambrian and Paleozoic strata below [*Xinjiang BGMR*, 1981d; *Liu*, 1988; *Xinjiang BGMR*, 1993]. The age of the Tertiary basin bounded by the thrusts is Eocene-early Oligocene based on preserved fossils in the strata [*Xinjiang BGMR*, 1981d]. The basin development is most likely related to motion along the two bounding thrusts, suggesting that the Jinyan and Xorkoli thrusts are Eocene-Oligocene in age. The inferred Paleogene age for the Jinyan thrust is consistent with the field observation that the fault is folded and is therefore no longer active (Figure 5).

[20] The hanging walls of the two Paleogene thrusts consist of garnet-bearing Proterozoic schist and marbles,

(A)

(C)

(B)

(D)
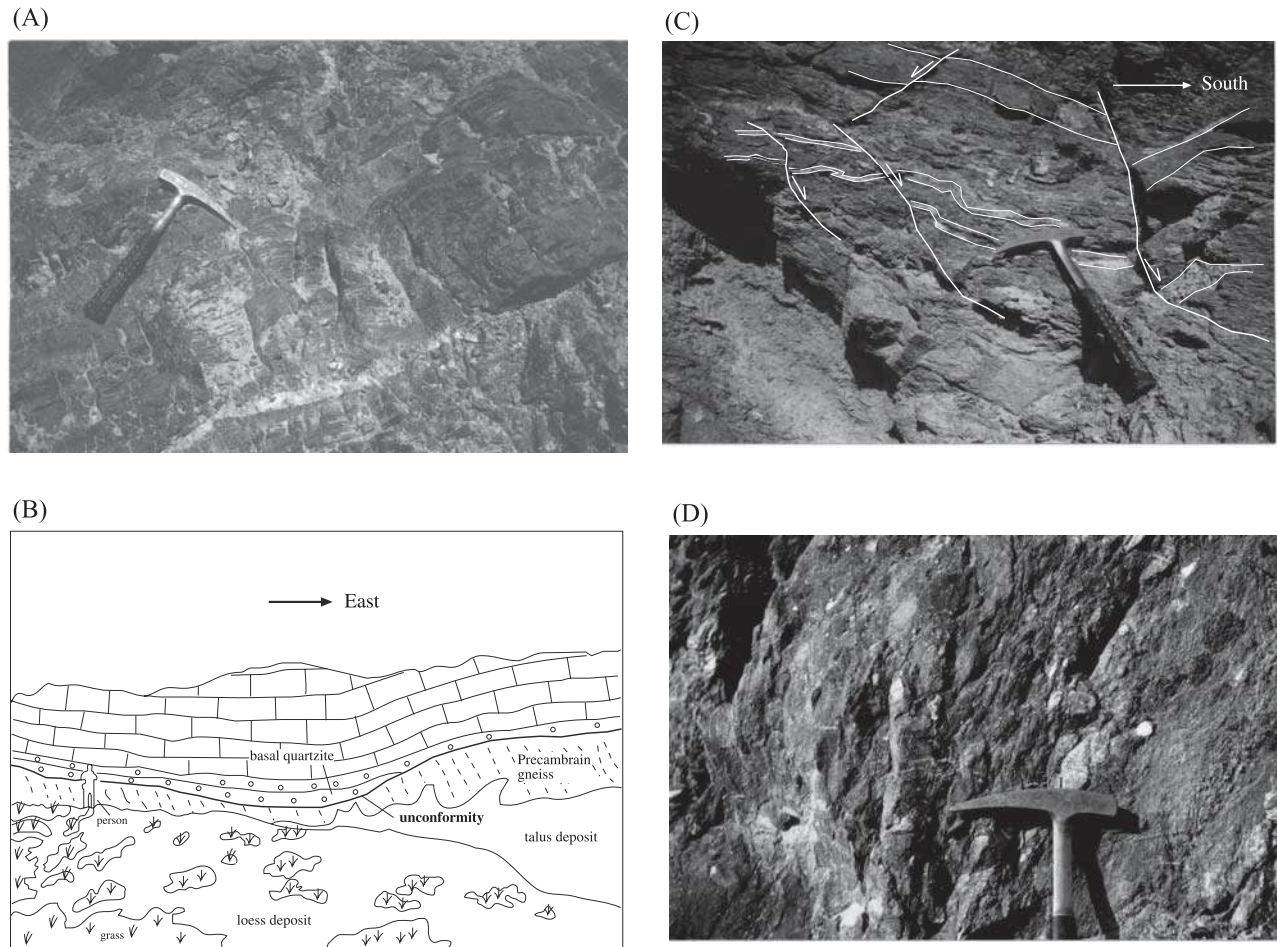
Figure 4. Field relationships. (a) Proterozoic stramatolite-bearing, cherty limestone in Annanba in the footwall of the Lapeiquan fault; see Figure 3 for location. (b) Sketch of unconformity between Proterozoic strata and Precambrian basement based on photo; see Figure 3 for location. (c) Minor normal faults and south verging asymmetric folds in Ordovician volcanic rocks directly above the Lapeiquan fault; see Figure 5 for location. (d) Jurassic basal conglomerates immediately above the unconformity. Dark gray colored cobbles are derived from the underlying Ordovician volcanic rocks, whereas white and purple colored cobbles are quartzite that match the lithology of Annanba Proterozoic sequence in the footwall of the Lapeiquan fault. See Figure 5 for location. (e) Jurassic strata directly above Figure 4d with clasts of stramatolite-bearing cherty limestone and purple quartzite. They match the lithology of Annanba Proterozoic sequence. The section is younging to the left (east). Note that the imbricated pebbles show southward paleocurrent direction. See Figure 5 for location. (f) Jurassic strata directly above exposure in Figure 4e. The clasts and cobbles are dominated by stramatolite-bearing limestone. See Figure 5 for location. (g) Asymmetric boudinages in the Lapeiquan ductile shear zone in the Kaladawan area; see Figure 6 for location. (h) Small conjugate normal faults above the south dipping Qiashikan fault in the Kaladawan area. See Figure 6 for location.

Ordovician volcanic and sedimentary rocks, Carboniferous limestone, and Jurassic conglomerates. As discussed below, the Lapeiquan fault is a Mesozoic normal fault. Thus, the Tertiary thrusts in the Lapeiquan area are interpreted to cut the Lapeiquan fault at depth on cross-sectional view (Figure 5). The Tertiary thrusts are in turn truncated by the younger left-slip Altyn Tagh fault in the east (Figure 5). The timing, evolution, and regional implication of the truncational relationship between the Tertiary thrust belt in the eastern Altyn Tagh range and the Altyn Tagh fault was briefly mentioned in *Yin and Harrison* [2000] and will be discussed fully elsewhere.

[21] The Lower and Middle Jurassic sedimentary rocks of *Xinjiang BGMR* [1981d] in the hanging wall of the Lapeiquan fault is a fining upward sequence consisting of conglomerate, course grained sandstone, siltstone, and coal-bearing shale. The contact between the Jurassic strata and the Ordovician volcanics is an angular unconformity. The Ordovician strata below are folded with amplitudes of 30–50 m and wavelengths of 30–50 m. Folds are best

(E)

(F)

Figure 4. (continued)

defined by the easily traceable massive blue limestone layers. The basal Jurassic conglomerate is about 50–60 m thick. In the lower 10–20 m section, it is dominated by cobbles of Ordovician volcanics with rare purple quartzite and stramatolite-bearing limestone (Figures 4d, 4e, and 4f). The amount of Ordovician volcanic clasts decreases rapidly up-section. At about 30–40 m above the basal contact, cobbles are dominated by cherty limestone, purple quartzite, and stramatolite-bearing limestone, all are characteristic for the Annanba shallow marine sequence (Figure 4d). Preliminary observations of pebble imbricates in this part of the Jurassic section indicate that the paleocurrent direction was from north to south (Figure 4e), which is consistent with the correlation between Jurassic clasts and Proterozoic strata in the Annanba area. However, at the top part of the 70-100 m conglomerate section, imbricate pebbles also indicate northward paleocurrent direction where volcanic clasts dominate again.

[22] The topmost part of the basal conglomerate sequence consists of a large landslide block, which is at least 200-m long and 20-m thick. The block is composed of a highly shattered gabbro body and relatively coherent basaltic layers. The landslide block, enclosed by Jurassic strata, could have been part of the Hongliugou suture that has been exhumed by the Lapeiquan fault in its footwall. The deposit of the landslide indicates significant topographic relief in the region at the time of Jurassic deposition. The above observations support the interpretation that the Jurassic strata in the Lapeiquan area were deposited during motion along the Lapeuiquan fault and extension in its hanging wall. This implies that the Lapeiquan fault was active in the Early Jurassic.

[23] Above the basal conglomerate that dips at 70°–80°S is a sequence of ∼200-m thick sandstones and shale that dip 10°–15° shallower. We interpret the upward shallowing in bedding dip to be induced by deposition of growth strata in a half graben, which was in turn controlled by a north dipping normal fault in the hanging wall of the Lapeiquan fault (Figures 5b and 5c). This interpretation can be tested by more detailed sedimentologic studies in the future. We cannot rule out the possibility that shallowing of Jurassic strata was induced by younger folding.

3.3. Kaladawan Area

[24] The Lapeiquan fault is most spectacularly exposed in this area. The fault zone is expressed by a 60–80-m thick ductile shear zone that juxtaposes an Early Paleozoic granite [*Xinjiang BGMR*, 1981d] in the hanging wall and an Archean-Proterozoic gneissic complex in the footwall [*Che and Sun*, 1996] (Figure 6). The Precambrian crystalline rocks consist of metabasite, foliated granite, and quartzo-feldspathic gneiss that are locally intruded by rare undeformed Paleozoic (?) granitic dikes (a few meters wide and tens of meters long). Granites in the hanging wall intrude into a sequence of basalt, andesite, marble, and graywacke which have been assigned an Early Paleozoic age [*Xinjiang BGMR*, 1981d]. The graywacke sequence is folded along east trending axes and its bedding is locally transposed by axial cleavage. South of the Lapeiqaun fault lies the Jinyan thrust that splits into two branches: its northern strand links with the Bashikaogong thrust to the west whereas its southern strand is covered by Quaternary alluvial fan deposits (Figure 2). Although the western segment of the Jinyan thrust puts Paleozoic strata over Tertiary sedimentary sequence, its western segment in the Kaladawan area juxtaposes younger Paleozoic graywacke unit over the older Proterozoic stramatolite-bearing marble (Figures 2 and 6). This unusual younger-over-older relationship suggests that the Tertiary Bashikaogong thrust may have originated either from an out-of-sequence thrust or from a north dipping normal fault that was later inverted to become a thrust. If the latter interpretation is correct, the Jinyan thrust could have been the inferred north dipping normal fault responsible for the deposition of the southward shallowing Jurassic strata in the Lapeiquan area (Figure 5c).

[25] The mylonitic shear zone immediately below the Lapeiquan fault consists of mylonitized marble, muscovite-biotite schist, and highly stretched granitoid boudins within a muscovite-biotite schist unit. Foliations strike east-west and dip at 60°–45°S. Stretching lineations are defined by
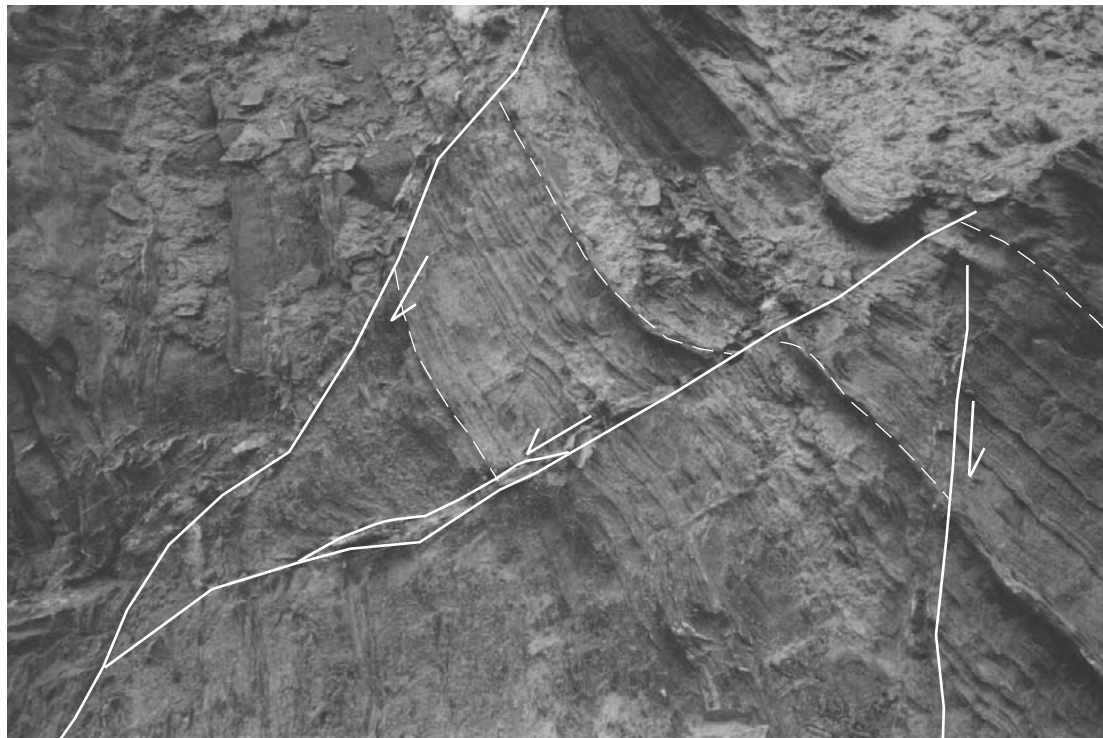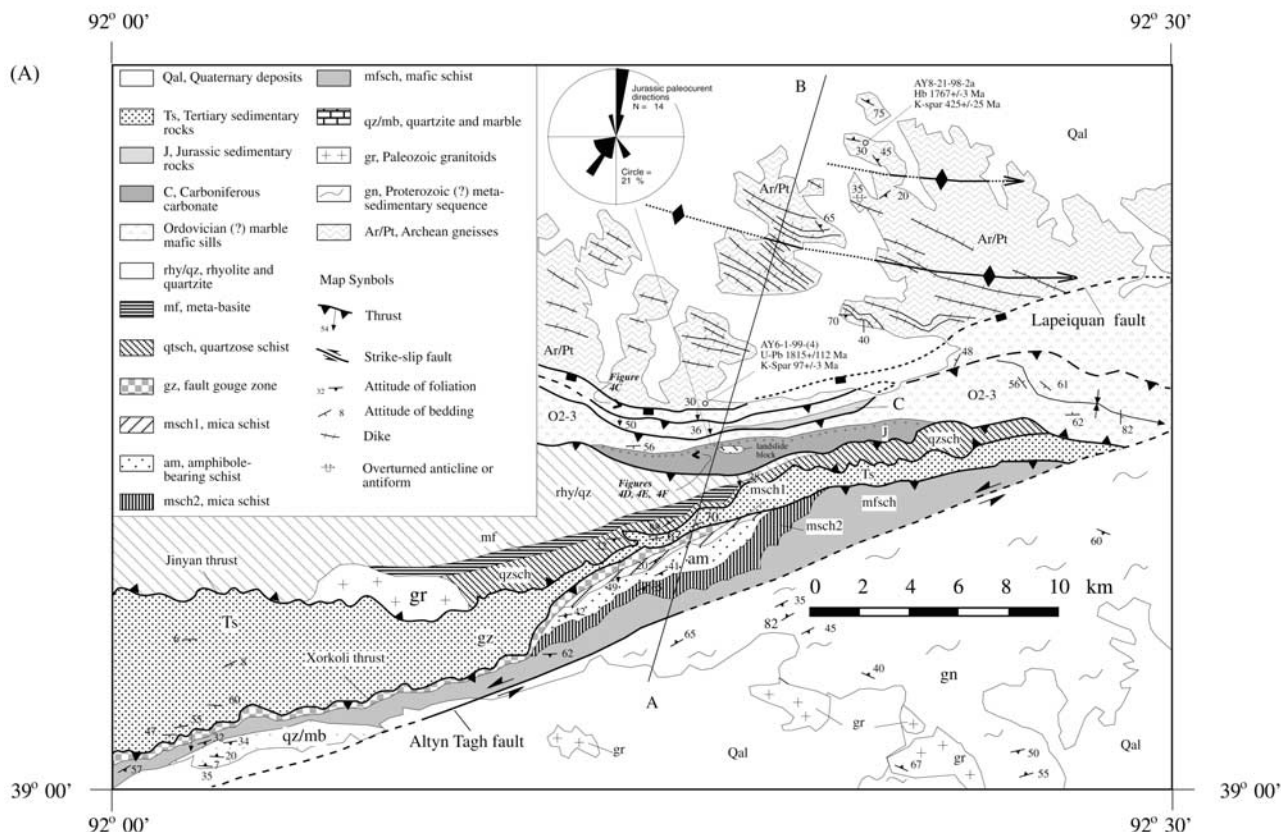
(G)

(H)

Figure 4. (continued)

Figure 5. (a) Geologic map of the Lapeiquan area based on our own geologic mapping at a scale of 1:100,000. See legends for map symbols. Location of Figure 5 is shown in Figure 2. (b) Geologic cross section (A-B) across the Lapeiquan area. (c) Schematic cross section showing possible relationship between Jurassic growth strata and Lapeiquan extensional fault system.

streaky quartz and broken plagioclase. Their trend is very close to the down-dip direction of the foliation (Figure 6b). The asymmetric boudinage consistently shows a top-south sense of shear (Figure 4g).

[26] In the hanging wall of the Lapeiquan fault, a south dipping fault, referred here as the Qiashikan normal fault in this study area, was mapped by *Xinjiang BGMR* [1981d] that puts an early Paleozoic graywacke sequence over an early Paleozoic granitoid (Figures 2 and 6). Along the traverse we investigated, the fault mapped by *Xinjiang BGMR* [1981d] is covered by a wash. Thus, we were not able to directly examine the kinematics of the fault. However, directly south of and above the inferred fault, mesoscopic normal faults are present in the graywacke units (Figure 4h). The concentration of small normal faults near the Qiashikan fault immediately south of its trace implies that the latter is probably an extensional structure. Based on the existing geologic map [*Xinjiang BGMR*, 1981d], knowledge of lithologic units in the mapped area, and the analysis of Landsat images, we interpret that the Qiashikan fault merges to the east with the Lapeiquan fault (Figure 6). The Qiashikan fault can be traced to the west to the Qiashikansayi area where the kinematic indicators in

the fault zone suggest it to be a normal fault (Figures 7a and 7b).

3.4. Qiashikansayi Area

[27] The easternmost exposure of the Lapeiquan fault was examined along the Qiashikansayi creek near Bashikaogong (Figures 2 and 7). The Lapeiquan fault here is defined by a cataclastic shear zone (>50 m thick) dipping ~30°–40° to the south. Its hanging wall consists of a sequence of folded volcanic, sedimentary, and metamorphic rocks. On the basis of lithology and the structural style we divide this study area into three geologic domains. The northern domain lies between the Lapeiquan normal fault in the north and the south dipping North Qiashikan thrust in the south. It consists dominantly of basalts interlayered with marble and quartzite beds. Locally conglomerates characterized by locally derived basaltic cobbles are also present. This unit is broadly folded. Bedding in this domain was transposed in places by the development of axial cleavage. The folded section is locally intruded by east trending mafic dikes of unknown age (Figures 7a and 7b). The North Qiashikan thrust juxtaposes a garnet-bearing gneissic unit
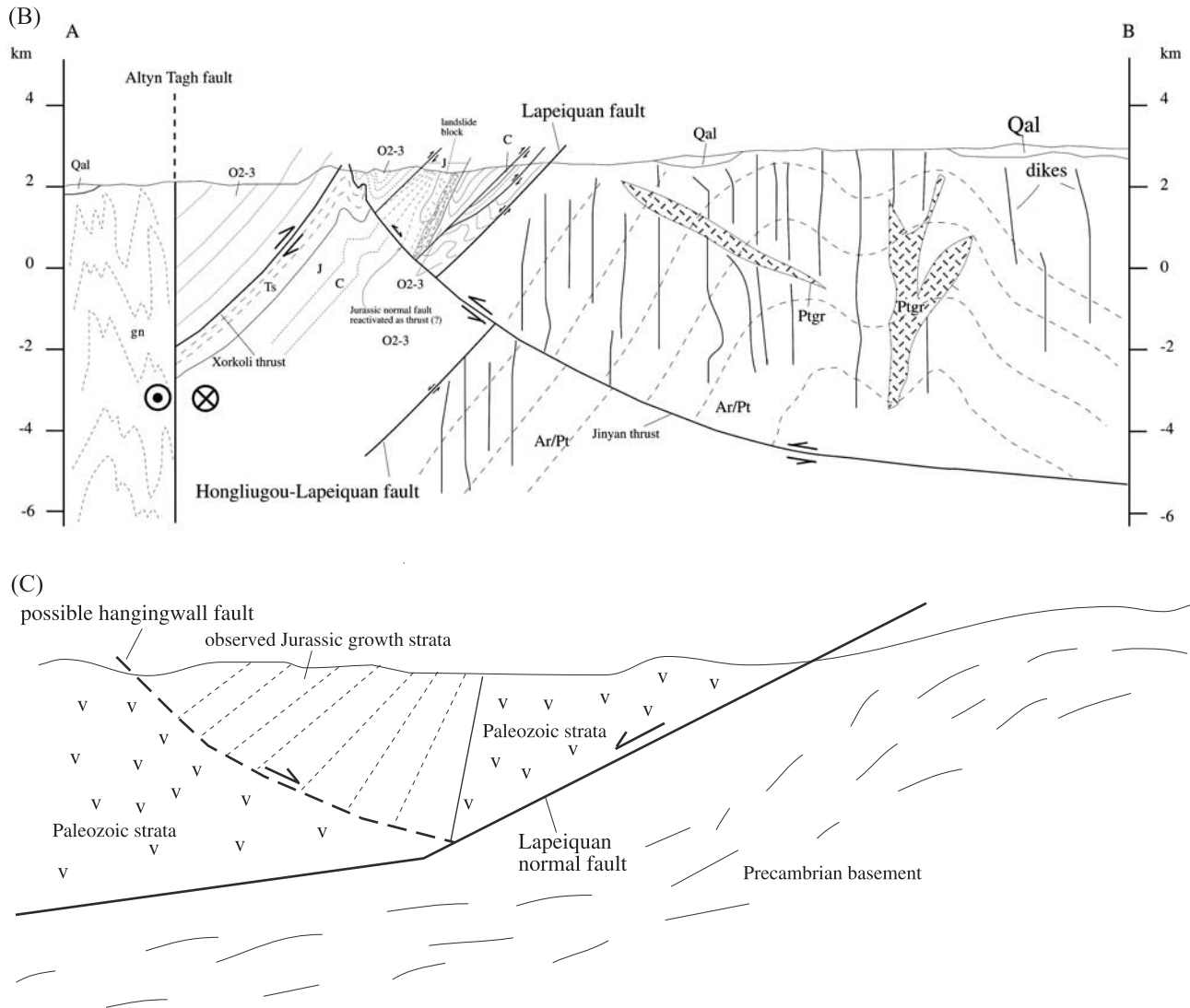
Figure 5. (continued)

over a sequence of north vergent isoclinal folds composed of find-grained sandstone and shale. The age and the magnitude of the North Qiashikan thrust are unknown.

[28] The central domain of the Qiashikansayi area consists of high-grade gneiss [*Che et al.*, 1995b; *Liu et al.*, 1999] and a melange complex that consists of ultramafic bodies [*Xinjiang BGMR*, 1986], abundant ribbon chert, and pillow basalts. The melange complex is presumably a part of the Hongliugou suture zone, first described by *Che et al.* [1995a, 1995b] and was extensively discussed later in the context of regional tectonics by *Sobel and Arnoad* [1999]. The boundary between the high-grade gneiss and the melange is a high-angle, south dipping ductile shear zone, here referred to as the Qiashikan normal fault. As shown by the existing geologic map [*Xinjiang BGMR*, 1981d, 1986] and via the analysis of Landsat images, this normal fault can be traced to the Kaladawan area where it merges with the Lapeiquan fault (Figures 2, 6, and 7).

[29] Directly below the south dipping Qiashikan normal fault is a ∼200-m thick zone of mylonitic gneisses (Figures 7a and 7b). The attitudes of the mylonitic foliations and lineations change systematically. Directly below the fault, the mylonitic foliation strikes east and dips steeply to the north. The corresponding lineations trend northwest. S-C fabrics indicate north-side-up and right-slip sense of shear. Further to the north, the mylonitic shear zone is dominated by south dipping foliations and south-plunging stretching lineations with down-to-the-south sense of shear as indicated by asymmetric folds, S-C fabrics, and en echelon quartz veins within the mylonitic gneiss. The lithologic units in the northern and central domains across the Qiashikan normal fault are similar, which are dominated by a basaltic sequence interbedded with limestone, mudstone, and siltstone (unit Pzb in Figures 7a and 7b). This duplication could have been caused by slip along either the Qiashikan normal fault or the North Qiashikan thrust.
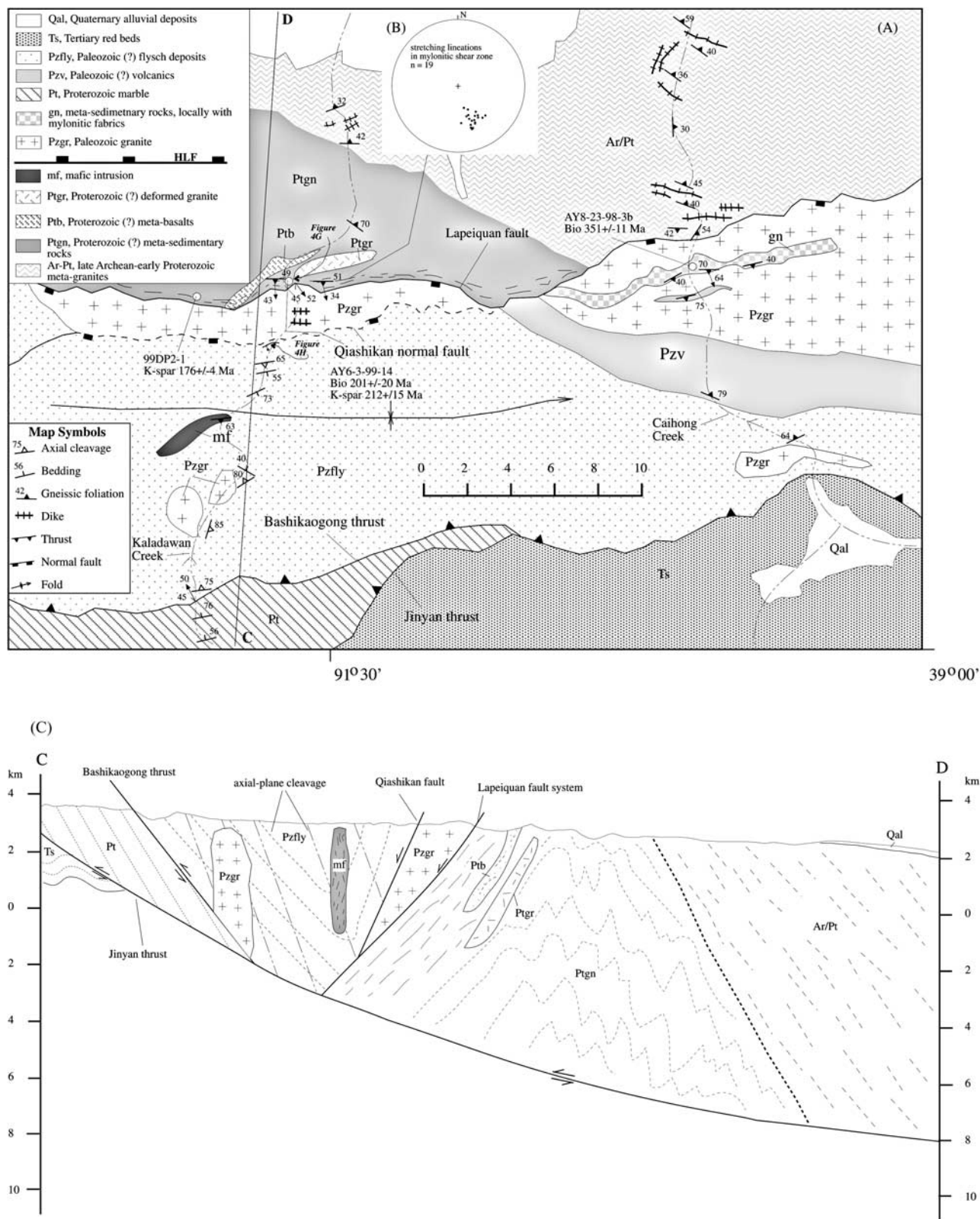
Figure 6. (a) Geologic map of the Kaladawan area and (b) stretching lineations of the mylonitic gneisses directly below the Lapeiquan fault. (c) Geologic cross section (C-D) of the Kaladawan area.
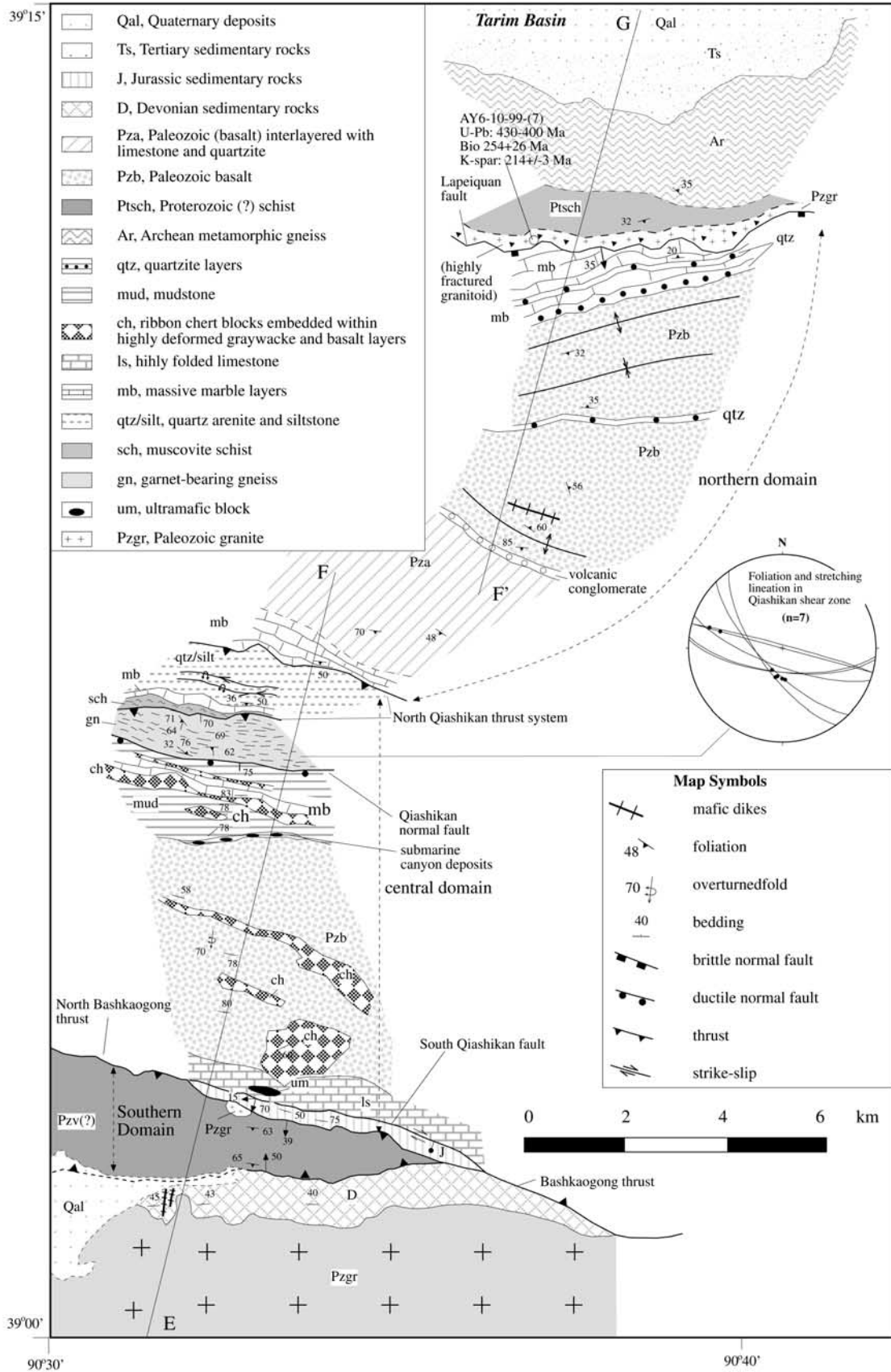
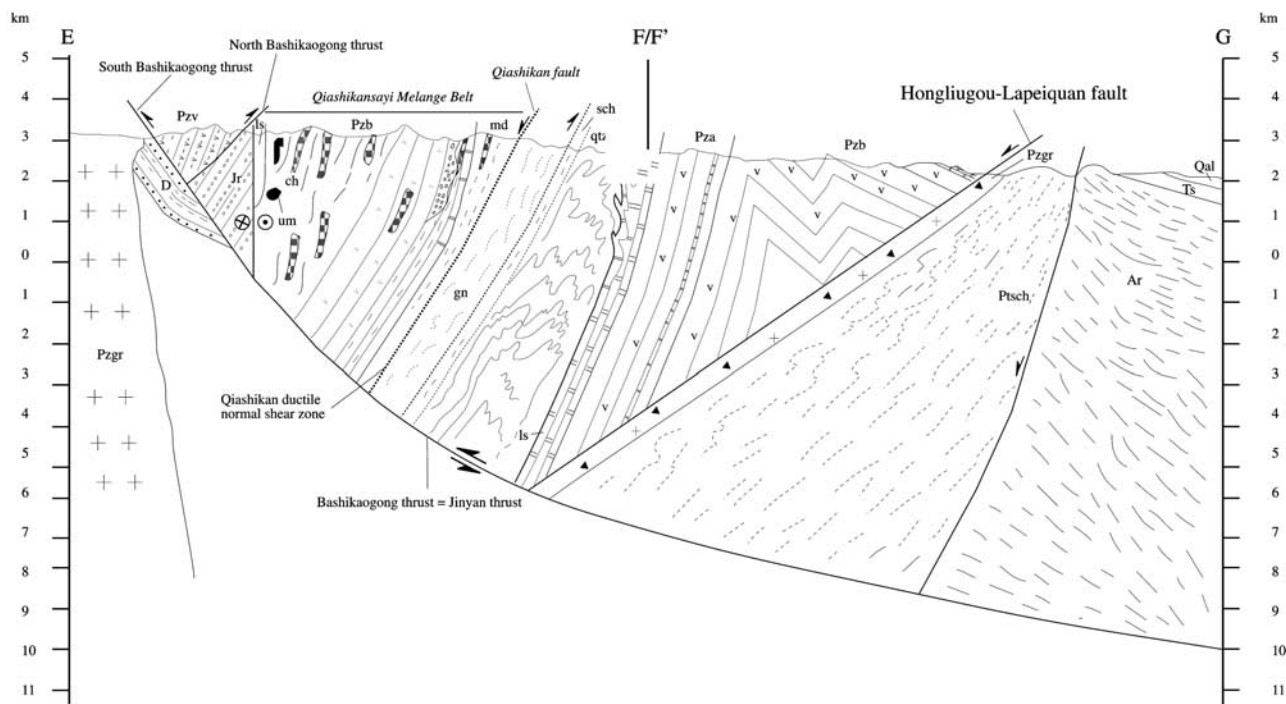**Figure 7a.** Geologic map of the Qiashikansayi area.

Figure 7b. Geologic cross section of the Qiashikansayi.

[30] The southern domain of the Lapeiquan hanging wall is a pop-up structure between the south dipping North Bashikaogong thrust and the north dipping Bashikaogong thrust. Both faults are Tertiary structures. This domain consists of a sequence of metavolcanic rocks, dominantly rhyolite and andesite that are intruded by small granitoids (Figure 7). The volcanic rocks were broadly assigned as early Paleozoic in age [*Xinjiang BGMR*, 1986]. The foot-wall rocks of the Bashikaogong thrust consist of a sequence of Devonian sandstone and shale intruded by a granitoid. A sliver of Jurassic strata is sandwiched between the North Bashikaogong thrust in the south and a brittle high-angle fault in the north (Figure 7). The Jurassic strata dip steeply to the south ($50°–75°$) and consist of ∼100-m thick conglomerate below and $20–30$ m thick coarse-grained sandstone. The clasts in the Jurassic strata are dominated by volcanics and purple quartzite. The former can be correlated with the Early Paleozoic volcanic rocks along the Qiashikansayi transect. The purple quartzite is charac-teristic of the Proterozoic cover sequence of the Tarim basement as we described in the Annanba area. Because of this correlation, we suggest that the Jurassic basin in the Qiashikansayi area also records unroofing history of the Tarim block in the footwall of the Lapeiquan fault. The similar dip direction and clast composition suggest that the Jurassic strata in the Qiashikansayi area may have been deposited in the same basin as Jurassic strata in the Lapeiquan area.

[31] The high-angle fault on the north side of Jurassic strata dips steeply to the southwest (∼70°) and is truncated by the Bashikaogong thrust at its eastern end. At one location, this fault is vertical and strikes N70°W. Striations on the fault surface plunge gently at 11°E. En echelon quartz veins within the fault zone suggest a right-slip sense of shear. From the crosscutting relationship, the right-slip fault here referred to as the South Qiashikan fault, we suggest that fault was active after deposition of the Jurassic strata and prior to the activation of the Tertiary Bashikao-gong thrust. The South Qiashikan fault is similar to the Qiashigan fault in their geometry and kinematics. Both dip steeply to the south and both have right-slip sense of motion. It is possible that the two faults were developed coevally.

[32] In the Qiashikansayi area, the Lapeiquan fault is characterized by a 10-20 m thick zone of cataclastic deformation. Because of the presence of well-developed fault gouge in the fault zone, striations are poorly devel-oped. Directly below the fault zone is a tabular-shaped early Paleozoic granitoid, $100–120$ m thick, which is extensively fractured and sheared. The granitoid may be a sliver in the fault zone (Figures 7a and 7b). Below the granitoid is a schist unit, assigned as Precambrian in age by *Xinjiang BGMR* [1986]. Well-developed foliation in the schist unit dips gently to the south ($30°–40°$), parallel to the dip of the Lapeiquan fault ∼150 m above. Numerous small-scale asymmetric folds (amplitude $= 3–5$ cm, and wavelength $= 5–10$ cm) are present within this unit. Those folds have east trending hinges parallel to the Lapeiquan fault and show a top-south sense of shear. The schist unit is juxtaposed against a gneiss unit by a south dipping high-angle brittle fault. We interpret this fault to be a member of the south dipping Lapeiquan normal fault system. Early Tertiary sedimentary strata at the northern end of our mapped area rest unconformably over the Precambrian

gneiss [*Xinjiang BGMR*, 1986]. The unconformity and the overlying early Tertiary strata dip gently to the north [*Xinjiang BGMR*, 1986], indicating the Lapeiquan fault and its footwall to have been tilted northward since early Tertiary. The kinematic indicators in the schist unit mentioned above and the observation that unmetamorphosed sedimentary and volcanic rocks overlying high-grade schist and gneiss support the interpretation that the Lapeiquan fault was an extensional structure.

4. Geochronology

[33] In order to better constrain the timing of slip along the Lapeiquan fault we have determined the crystallization ages and low-temperature thermal histories of several samples in the footwall. Ion microprobe U-Pb dating of zircon and $^{40}Ar/^{39}Ar$ dating of hornblende were performed to constrain crystallization ages while $^{40}Ar/^{39}Ar$ step-heating of K-feldspar yielded thermal history data. Tabulated results of the isotopic measurements and details of the analytical methods employed are available as auxiliary material[1].

4.1. U-Pb Geochronology

[34] Measurements were performed on three granitoid samples from the footwall of the Lapeiquan fault (AY6-10-99-(7), AY6-3-99-14, and AY6-1-99-(4)). A forth specimen (99DP2-1) yielded insufficient zircons for analysis. All errors quoted are ±1σ analytical uncertainties. Based on repeated analysis of AS-3 standard zircon (1099 Ma [*Paces and Miller*, 1993]) during the analysis of the above samples, our expectation is that their U-Pb age could be determined with a precision of better than 2.5% provided that they were homogeneous in age and contained uranium concentrations that were comparable to AS-3 (∼550 ppm).

[35] Sample AY6-10-99-(7) was collected from the highly fractured granitoid directly below the Lapeiquan fault in the Qiashikansayi area (Figure 7a). Five spots measured on five grains yielded essentially concordant ages between ca. 400–430 Ma (Figure 8a). The weighted mean $^{206}Pb/^{238}U$ and $^{207}Pb/^{235}U$ ages calculated from these results are 418 ± 8 Ma and 402 ± 16 Ma, respectively. We interpret these results to closely approximate the intrusive age of this granitoid and point out that its age is similar to those determined for other Paleozoic igneous rocks exposed along the Altyn Tagh fault to the southwest [*Cowgill*, 2001].

[36] Sample AY6-3-99-14 from the Kaladawan area (Figure 6a) yielded a more complex result. The sample is located about 200 m below the Lapeiqaun fault and represents an undeformed granitoid dike intruded into Proterozoic metasedimentary and metavolcanic rocks. Five spot analyses from five grains yielded a wide range of discordant results between 100–415 Ma (Figure 8b). We interpret this dispersion of U-Pb ages to have resulted from Pb loss and note that the oldest age obtained was approximately con-

cordant at 413 ± 7 Ma. The age similarity of this result to the crystallization age determined for sample AY6-10-99-(7) indicates the likelihood that the granitic dike is also part of a widespread early Paleozoic intrusive sequence in northern Tibet [*Cowgill*, 2001]. The presence of Paleozoic granites in the footwall of the Lapeiquan fault is a new discovery, because the age of this terrane was previously regarded late Archean. The lack of Paleozoic plutons in the Tarim basement has been used as evidence for the presence of a south dipping subduction zone in the early Paleozoic [*Sobel and Arnoad*, 1999]. However, our results appear to be inconsistent with this simple model.

[37] The final sample, AY6-1-99-(4), was collected immediately adjacent to the Lapeiquan fault from a granitic gneiss as part of the Precambrian basement rocks in the footwall (Figure 4a). Spot analyses obtained from zircons in this specimen are also widely dispersed and discordant in a manner consistent with a discrete episode of Pb loss (Figure 8c). A best fit line to all data points yields a well-defined upper intercept of 1815 ± 12 Ma with concordia. The lower intercept of the array of U-Pb results from AY6-1-99-(4) (133 ± 15 Ma) is slightly older than the time of rapid cooling recorded by coexisting K-feldspar (see next section). We also analyzed hornblende from a lithologically similar sample (AY8-21-98-2A) situated about 12 km north of the Lapeiquan fault (Figure 4). The total gas age yielded by this sample, 1767 ± 3 Ma (see next section), is only slightly younger than the upper intercept U-Pb age determined for zircons from AY6-1-99-(4).

4.2. $^{40}Ar/^{39}Ar$ Thermal History Results

[38] A total of five K-feldspars from the footwall of the Lapeiquan fault were step-heated by the $^{40}Ar/^{39}Ar$ method to determine cooling histories immediately adjacent to, and distal from the fault (Figure 9). The results were interpreted using the multi-diffusion domain (MDD) model [*Lovera et al.*, 1989] using the assumption of slow-cooling. The approach employed is discussed by *Lovera et al.* [1997]. Details of the modeling process employed with the samples examined in this paper employed can be obtained from the electronic supporting material. Note that in the case of sample AY9-21-98-2A (Figure 9i), it was necessary to correct for the initial portion of its age spectrum for Cl-correlated excess radiogenic ^{40}Ar [*Harrison et al.*, 1994]. While the other samples did not require such treatment, other features of their age spectra are problematic and require detailed discussion.

[39] Many, though not all, K-feldspars sampled within high-strain zones proximal to faults exhibit intermediate age maxima that signal partial failure of the underlying assumptions of the MDD model and hence limit detailed interpretation of thermal histories obtained from them [*Lovera et al.*, 2002]. All five samples obtained adjacent to the Lapeiquan fault exhibit these features (see Figures 9a, 9c, 9e, 9g, and 9i). The most prominent example is yielded by AY6-3-99-14 K-feldspar (Figure 9e). The possible origin and significance of intermediate age maxima in K-feldspar age spectra are discussed in *Lovera et al.* [2002]. While this topic is beyond the scope of this paper, it is most important

---

[1] Auxiliary material is available via Web browser or via Anonymous FTP from ftp://ftp.agu.org/apend/tc/2001TC001336. Information on searching and submitting electronic supplements is found at http://www.agu.org/pubs/esupp_about.html.

to point out that the existence of the features limits our ability to accurately recover thermal histories from the samples. In spite of this limitation, the unaffected portions of the age spectra are quite simple to interpret and we have proceeded on these grounds.

[40] Three K-feldspars obtained from Paleozoic granitoids distributed along the western portion of the Lapeiquan fault yield broadly similar results. These include samples 99DP2-1 and AY6-3-99-14 from the Kaladawan area (Figure 6a) and AY6-10-99-(7) from the Qiashikansayi area (Figure 7a). All three samples reveal pronounced age gradients between 100-200 Ma and flat age spectra at high temperature stages of cumulative ^{39}Ar release defined by ca. 186 Ma ages for sample 99DP2-1 (Figure 9a) and circa 220 Ma ages for samples AY6-10-99-(7) (Figure 9c) and

AY6-3-99-14 (Figure 9e). In applying the MDD model approach to these samples, we neglected the intermediate age maximum that typically affects the age spectrum between about 15–25% cumulative ^{39}Ar release and assumed monotonic cooling. The resulting thermal histories, represented by 90% confidence intervals for the mean of 50 best fit solutions, are shown in Figures 9b, 9d, 9f, 9h, and 9j, respectively. The corresponding best fit age spectra are shown in Figures 9a, 9c, 9e, 9g, and 9i. Despite the fact that detailed interpretation of the thermal history results is likely to be problematic, we are struck by the similarity of the results and suggest that it is likely that all samples experienced rapid cooling to below 200°C between 220–185 Ma and slower cooling at upper crustal levels for the next 80 m.y.

[41] Further to the east, two K-feldspars were analyzed from the Lapeiquan area (Figure 4). As discussed above, both samples were collected from the Precambrian gneisses. The age spectrum obtained from the sample adjacent to the Lapeiquan fault, AY6-1-99-(4), yields an age gradient from ca. 30 Ma to 100 Ma over the initial 15% of ^{39}Ar release and a flat age spectrum defined by 100 Ma ages thereafter (Figure 9g). Following the same type of analysis outlined above, these results indicate rapid cooling to below ~175°C at 100 Ma followed by slow cooling into the Late Oligocene (Figure 9h). Further away from the Lapeiquan fault, sample AY8-21-98-2A (Figure 9i) indicates protracted slow cooling within the middle- to upper crust throughout the Paleozoic and early Mesozoic (Figure 9j). This result is consistent with the fission track analysis of a sample collected by *Sobel et al.* [2001] near the location of our sample AY8-21-98-2A, who showed that single grain zircons yielded an age of 221 ± 26 Ma and apatites yielded an age of 167 ± 15 Ma. Hornblende from sample AY8-21-98-2A yielded a total gas age of 1767 ± 3 Ma (see electronic supporting material). Because no major faults lie between samples AY6-1-99-(4)
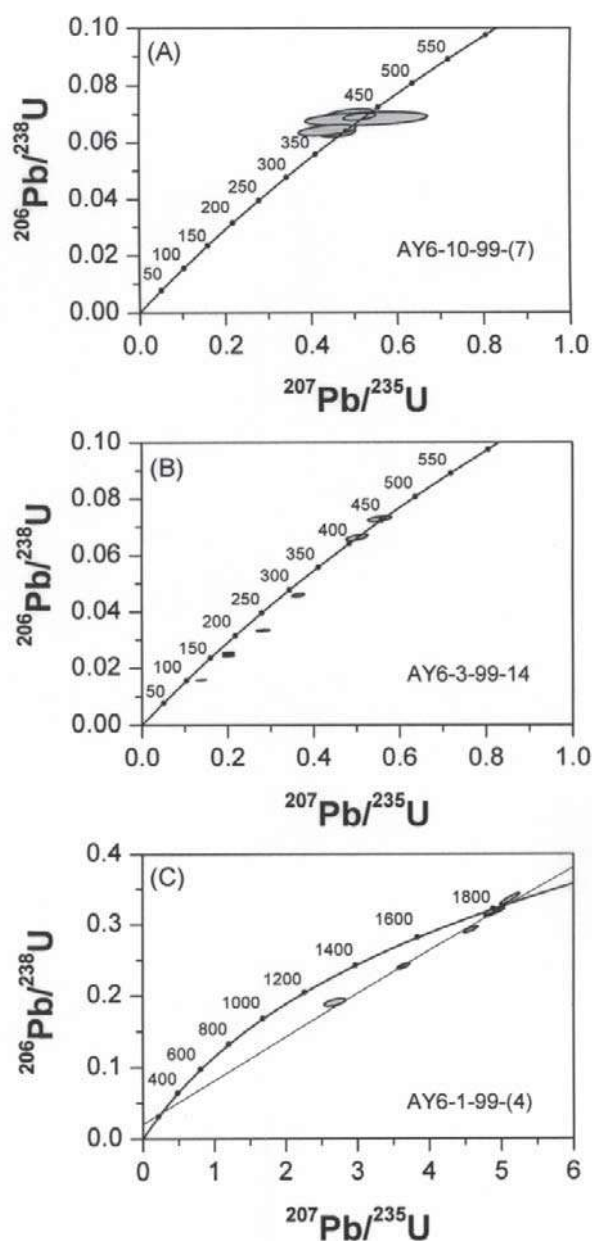
Figure 8. (opposite) Results of U-Pb dating of zircons. (A) Sample AY6-10-99-(7) from the highly sheared granitoid directly below the Lapeiquan fault in the Qiashikansayi area. Five spots measured on five grains yielded essentially concordant ages between ca. 400–430 Ma. The weighted mean ^{206}Pb/^{238}U and ^{207}Pb/^{235}U ages calculated from these results are 418 ± 8 Ma and 402 ± 16 Ma, respectively. (B) Sample AY6-3-99-14 from the Kaladawan area yielded a more complex result. The sample represents an undeformed granitoid dike intruded into Proterozoic metasedimentary rocks. Five spot analyses from five grains yielded a wide range of discordant results between 100–415 Ma. We interpret the dispersion ages of U-Pb ages to have resulted from Pb loss and note that the oldest age obtained was approximately concordant at 413 ± 7 Ma. (C) Result from sample AY6-1-99-(4). Spot analyses obtained from zircons in this specimen are widely dispersed and discordant in a manner consistent with a discrete episode of Pb loss. A best fit line to all data points yields a well-defined upper intercept of 1815 ± 12 Ma with concordia. The lower intercept (133 ± 15 Ma) is slightly older than the time of rapid cooling recorded by coexisting K-feldspar for the same sample.
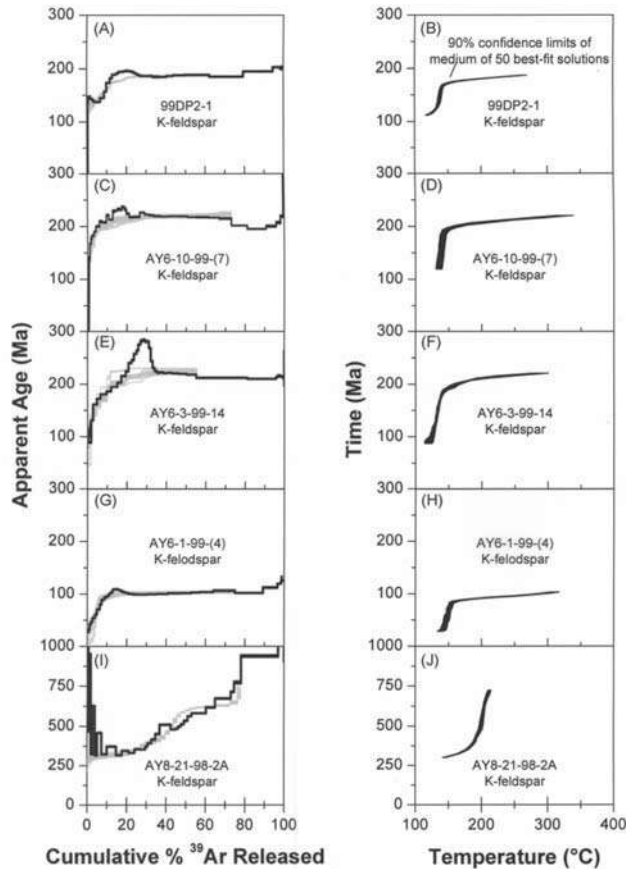
Figure 9. Results of multi-diffusion-domain analysis of K-feldspars using the $^{40}Ar/^{39}Ar$ step-heating method. Graphics (A), (C), (E), (G), and (I) are measured (solid lines) and modeled (light gray lines) age spectra for samples 99DP2-1, AY6-10-99-(7), AY6-3-99-14, AY6-1-99-(4), and AY8-21-99-2A. Graphics (B), (D), (F), (H), and (J) are calculated cooling histories of the five samples.

and AY8-21-98-2A, the contrast in thermal histories (>150°C at 100 Ma) requires that the present exposure levels of Proterozoic gneiss exposed along the Lapeiquan fault originated from a depth at least 5 km deeper than those 10 km to the northeast. This is consistent with our field observation indicating that the south dipping Lapeiquan fault is a normal fault. That is, the fault cuts progressively deeper to the south.

[42] Total gas ages of biotite are also obtained from this study, although they all yielded large uncertainties. In the Kaladawan area, a biotite age of 351 ± 11 (2σ) Ma were obtained from a gneiss unit in the Lapeiquan hanging wall (AY8-23-98-3b, Figure 6). This is in contrast to a younger biotite age of 201 ± 20 (2σ) Ma obtained from a Paleozoic dike in the footwall (AY6-3-99-14, Figure 6). The cooling age of biotite in the footwall is similar to the duration of rapid cooling inferred from K-feldspar analysis. The contrasting cooling ages of biotite across the fault again support the interpretation that the Lapeiquan fault is a normal-slip

structure. In the Qiashikansayi area, a biotite age of 254 ± 26 Ma (2σ) is obtained from the Paleozoic granite in the Lapeiquan footwall (Figures 7a and 7b). This age suggests that cooling of the early Paleozoic granite could have started as early as Early Triassic, which may imply that extension in northern Tibet may have started earlier than that indicated by the results of K-feldspar analyses.

5. Discussion

5.1. Timing and Structural Development of the Lapeiquan Normal Fault

[43] The most interesting result from the $^{40}Ar/^{39}Ar$ thermochronologic studies is the discovery of two episodes of rapid cooling in the footwall of the Lapeiquan fault. The first occurred in the early Jurassic at ~187–200 Ma along the central and western segments of the fault, and the second in the latest Early Cretaceous at ~100 Ma along the eastern segment of the fault. This finding appears to be puzzling at first, because it requires very different movement histories along the same fault. However, this problem can be resolved when considering the Qiashikan fault as a younger element of the Lapeiquan fault system. The south dipping Qiashikan fault merges with the Lapeiquan fault just east of the Kaladawan traverse (Figure 2). This relationship suggests that the eastern segment of the Lapeiquan fault could have moved together with the Qiashikan fault in the Cretaceous while the western Lapeiquan fault was inactive. The age of the Qiashikan fault is unknown, but the above geometrical interpretation on the relationship between the Qiashikan and Lapeiquan faults implies that the two must be synchronous. This leads to the possibility that the Lapeiquan fault was initially an Early Jurassic normal fault and was later reactivated by motion along the Qiashikan-eastern Lapeiquan fault in the Cretaceous (Figure 10a). Alternatively, the younger Qiashikan fault may have cut and offset the older Lapeiquan fault (Figure 10b). The lack of prominent faults in the footwall of the eastern Lapeiquan fault, as indicated by the continuation of northwest trending dike swarms in the Precambrian crystalline basement, support the first possibility. If the Qiashikan fault is a Cretaceous fault, its magnitude of vertical offset must be relatively small along the Qiashikansayi traverse. Muscovites from the high-grade gneiss immediately below the Qiashikan normal fault yielded $^{40}Ar/^{39}Ar$ cooling ages of 575 ± 3 Ma and 573 ± 6 Ma [*Liu et al.*, 1999]. This means that the magnitude of Cretaceous normal faulting was not sufficient to reset the muscovite cooling ages.

[44] The interpretation that the Lapeiquan fault was active in the Early Jurassic is consistent with the observation that the Lower and Middle Jurassic strata in the hanging wall of the Lapeiquan fault were deposited in a half-graben basin with its proximal clasts derived from both its footwall and hanging wall. We also note that Middle Jurassic alkaline basalts are common in the northern Altyn Tagh area, as recently reported by *Guo et al.* [1999] and *Zhang et al.* [1998] at Tuoge, Duobagou, and Lucaogou localities (Figure 1). The age of the basalts was constrained by interbedded sedimentary strata which contain plant
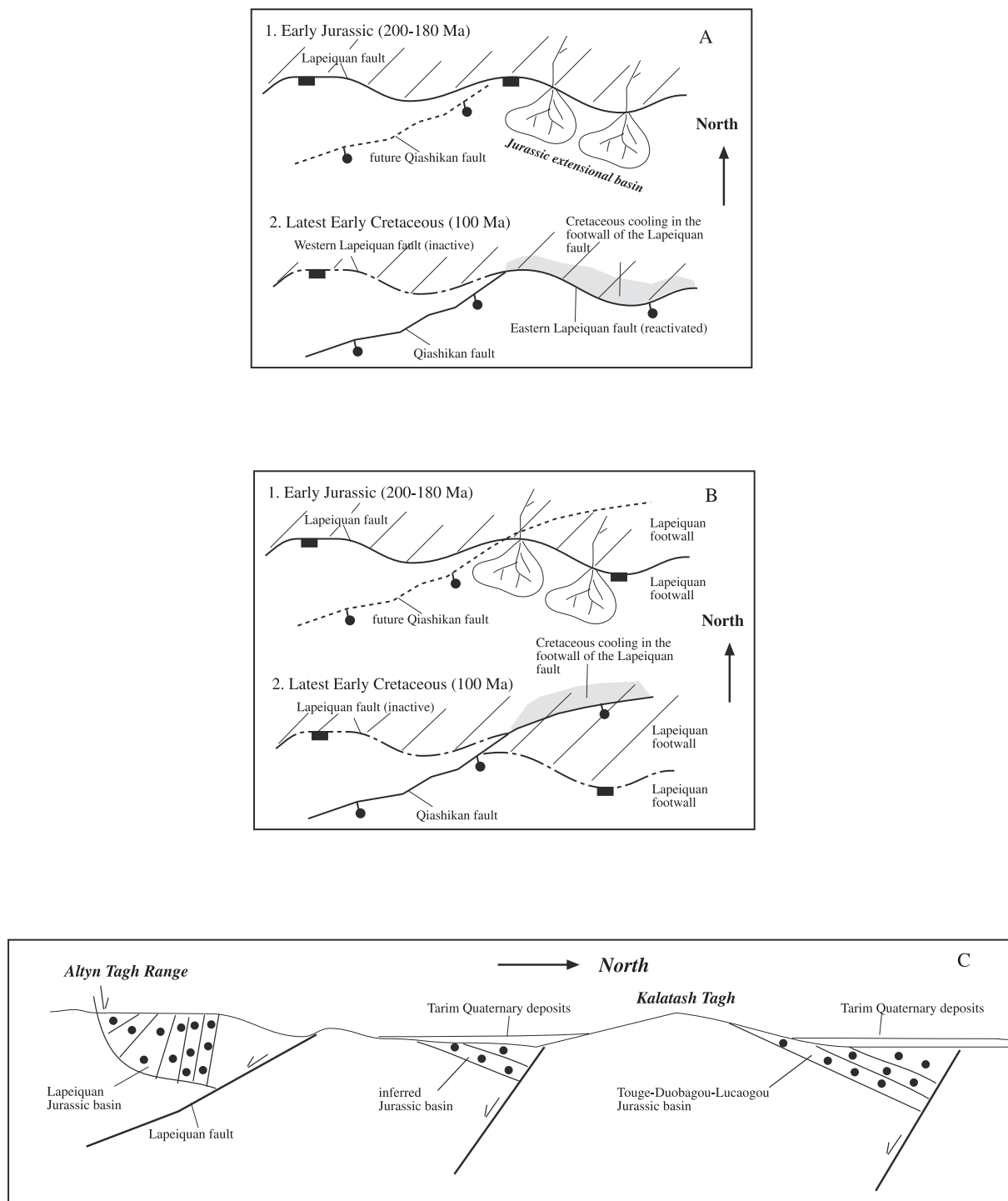
Figure 10. Two possible models for the relationship between the Lapeiquan and Qiashikan normal faults. (A) The Qiashikan fault reactivates the eastern segment of the Early Jurassic Lapeiquan fault in the Cretaceous. This model predicts Cretaceous cooling immediately below the footwall of the eastern Lapeiquan fault as documented by this study. (B) The Qiashikan fault cut and offset the Early Lapeiquan fault in the Cretaceous. This model predicts that Cretaceous cooling history should be recorded in the footwall of a major fault within the Precambrian gneiss in the footwall of the Lapeiquan fault, which has not been observed. (C) Schematic cross section illustrating possible style of Jurassic deformation and sedimentation in northern Altyn Tagh and southern Tarim. Note that Early and Middle Jurassic strata are deposited in half-grabens controlled by domino-style normal faults.

fossils of *Sphenobaierd* sp., *Cladophlebis* sp., and *Pityophylam* sp. The Middle basaltic volcanism in the northern Altyn Tagh region may be related to extensional event in the eastern Altyn Tagh range as we reported here. The reoccurrence of Middle Jurassic strata in the footwall of the Lapeiquan fault in the southernmost Tarim basin also suggests that Early-Middle Jurassic basins were partitioned by multiple normal faults, perhaps in a domino-style extensional system (Figure 10c).

[45] The interpretation that Lower and Middle Jurassic (208–163 Ma) strata in the Altyn Tagh region were related to extension differs drastically from the traditional view that contraction was dominated at this period [e.g., *Huo and Tan*, 1995]. *Ritts and Biffi* [2000] recently amplified this view by suggesting that the Lower and Middle Jurassic strata along the central and eastern Altyn Tagh fault to have deposited in a single large lake in a foreland basin setting controlled by a north directed thrust belt in the Kunlun Shan. The sparse Jurassic outcrops used in that study, the lack of direct ties between deposition of the Jurassic strata they studied with any known Jurassic faults make their simple interpretation unattainable. Simply put it, there might be numerous Jurassic basins in northern Tibet isolated from one another and controlled by local normal faults as in the eastern Altyn Tagh range. Under this scheme, correlating Jurassic shoreline facies an approach adopted by *Ritts and Biffi* [2000] across the Cenozoic Altyn Tagh fault may not yield useful offset markers. It is interesting to note that Early Jurassic cooling ages are widespread throughout the Altyn Tagh massif [*Cowgill*, 2001; *Sobel et al.*, 2001]. Although this cooling event was interpreted to have been related to contraction [*Sobel et al.*, 2001], the results of our structural observations strongly suggest that these cooling ages too could have been related to extensional tectonics. This means that the sporadic outcrop of Lower and Middle Jurassic strata on both sides of the Altyn Tagh fault in northern Tibet could have been deposited in numerous half-graben basins controlled by extensional faults. Thus, correlating Jurassic lake shorelines across the Altyn Tagh fault as offset markers may require a greater deal of care than the simple approach adopted by *Ritts and Biffi* [2000]. The effect of Mesozoic exhumation along the northern margin of the Tibetan Plateau has also been detected in sandstone composition of Tertiary strata in southern Tarim. As reported by *Yin et al.* [2002], the primary provenance of Tertiary sediments is the Paleozoic volcanic and sedimentary strata exposed along the northern margin of the Tibetan plateau. Due to the lack of detrital clasts from the Mesozoic strata in the Tertiary sections and the similarity of sandstone modal composition between Jurassic-Cretaceous and Tertiary strata, *Yin et al.* [2002] suggest that a significant denudation event occurred in the Late Triassic and Early Jurassic in northern Tibet. This conclusion is consistent with the timing of the first extensional event in the eastern Altyn Tagh range documented in this study.

[46] *Sobel* [1999] interpreted the lower Middle Jurassic strata in the western Kunlun as having been deposited in a transtensional basin controlled by a strike-slip system. The inferred trend of that basin is northwest. The western Kunlun Shan has been rotated clockwise during Cenozoic

northward indentation of the Pamir massif [*Burtman and Molnar*, 1993; *Rumelhart et al.*, 1999; *Shen et al.*, 2001]. Thus the Jurassic basin studied by *Sobel* [1999] may trend nearly east-west at the time of its formation as a result of north-south extension. This interpretation implies that Early-Middle Jurassic extension may be widespread in northern Tibet.

[47] Late Jurassic to Early Cretaceous extension has been well known in the Jiuquan basin where the Altyn Tagh fault meets the Qilian Shan thrust front as a result of several decades of petroleum exploration [*Huo and Tan*, 1995] (Figure 1). In seismic reflection profiles through the basin, numerous normal faults either in the domino style control growth strata involving Late Jurassic to Early Cretaceous strata. *Vincent and Allen* [1999] investigated Triassic to Early Cretaceous strata in the Minle and Chaoshui basins east of the Jiuquan basin. They inferred the two basins to have developed in a pull-apart setting in the Early Cretaceous associated with two east striking right-slip faults bounding the basins. Although they present no structural evidence to support the presence of right-slip faults in the Jiuquan region, the east striking right-slip South Qiashikan fault we mapped in the Qiashikansayi could be part of this inferred Cretaceous right-slip system when 280-km left-slip motion along the Cenozoic Altyn Tagh fault is restored.

[48] The duration of extension in the Late Jurassic and Early Cretaceous in the Jiuquan basin lies between the two phases of extension we document in the eastern Altyn Tagh range. This may suggest that extensional tectonics may have been a continuous process between the Early Jurassic and Early Cretaceous in northern Tibet, although the life span of individual extensional structures may have been short and diachronous. We also note that Cretaceous extension in the Jiuquan basin was associated with two episodes of basaltic eruption at 112–106 Ma and 82 Ma [*Yang et al.*, 2001]. Although the tectonic setting in the Late Cretaceous is uncertain in northern Tibet, the region was under contractional deformation soon after the initial collision between India and Asia at ~65–55 Ma [*Horton et al.*, 2002; *Yin et al.*, 2002].

[49] Widespread Early to Middle Jurassic extension in northern Tibet appears at odds with the hypothesis of *Hendrix et al.* [1992] that the Tian Shan was experiencing contractional deformation at the time as induced by collision between the Qiangtang and Lhasa terranes from the south. It is also important to note that there has been no direct structural evidence to support Jurassic contractional tectonics in the Tian Shan. Thus the nature of Jurassic structural setting of the Tian Shan remains an open question.

5.2. Jurassic and Cretaceous Tectonic Settings of Northern Tibet and Eastern Asia

[50] An obvious question raised by this study is what caused two phases of Mesozoic north-south extension in the northern Tibetan plateau. During the Late Triassic collision among the Qiangtang, Songpan-Ganzi, Kunlun, and North China terranes a broad orogenic belt formed in northern Tibet [*Hsü et al.*, 1995; *Yin and Harrison*, 2000]. In the

early Jurassic the southern edge of the Qiangtang terrane was the southern margin of the Asian continent. It appears that a north dipping subduction zone was immediately established along the southern margin of the Qiangtang as soon as the collision between the Qiangtang and the Kunlun terranes were completed [*Yin and Harrison*, 2000]. The presence of this magmatic arc is indicated by the Late Triassic-Early Jurassic granitic intrusion [*Kapp et al.*, 2000] and widely distributed andesitic flows in the Qiangtang terrane [*Cheng and Xu*, 1986]. These observations suggest that the Jurassic Altyn Tagh range lie behind an arc. Widespread extension also occurred in the Qiangtang terrane in the earliest Jurassic at ∼200 Ma [*Kapp et al.*, 2000]. However, the Qiangtang extensional system is entirely located within the Jurassic arc and its extensional direction is east-west, orthogonal to what we observed in the eastern Altyn Tagh region.

[51] Mesozoic intracontinental extension is widespread in east Asia, although the cause for such widely distributed extension and the pattern of complex temporal and spatial association with contractional deformation remain subjects of intense investigations and debate in recent years [*Yin and Nie*, 1996; *Ratschbacher et al.*, 2000; *Davis et al.*, 2001a, 2001b; *Graham et al.*, 2001; *Ren et al.*, 2002]. However, Early to Middle Jurassic extension is relatively rare in central and eastern Asia (see *Graham et al.* [2001] for a summary). Two Early Jurassic extensional systems that have been firmly established so far are located in southeast Siberia near Lake Baikal [*Zorin*, 1999] and in the Daqing Shan of northern China [*Darby et al.*, 2001]. These extensional systems, active in relatively short time spans and separated widely in space, may not have been active coevally all together [*Graham et al.*, 2001].

[52] Early Cretaceous extension in northern Tibet is coeval with the development of a thin-skinned fold-thrust belt in the Lhasa block while it was continuously converging with the Qiangtang block [*Yin et al.*, 1994; *Murphy et al.*, 1997]. This tectonic setting suggests that Cretaceous extension in northern Tibet may have been related to collision between the Lhasa block and Asia leading to eastward extrusion associated back arc extension behind the Pacific subduction zone [*Ratschbacher et al.*, 2000]. However, because the Gangdese batholith was also developing at this time along the southern edge of Tibet and Asian margin [*Yin and Harrison*, 2000], the Cretaceous extensional systems in northern Tibet may be treated as a back arc process. The coeval Cretaceous basaltic eruptions are spatially associated with the northern Tibet extensional systems in the eastern Altyn Tagh range and the Jiuquan basin. This may indicate that extension involves mantle lithosphere, and thus precludes gravitational spreading of an overthickened crust as the only cause for the development of the Cretaceous normal faults.

5.3. Relationship Between Mesozoic and Cenozoic Structures

[53] The Lapeiquan fault is cut by the Altyn Tagh fault. Thus, its development did not affect the initiation and development of this major intracontinental strike-slip fault. However, Mesozoic extensional structures may have played a role in controlling smaller-scale structures. For example, the Bashikaogong thrust locally puts younger Paleozoic strata over Proterozoic strata (Figure 6) which could be explained by inversion of an older Mesozoic north dipping normal fault. Because the effect of Cenozoic deformation has not been removed, a complete palinspastic reconstruction of Mesozoic northern Tibet remains premature.

6. Conclusions

[54] The >300-km long, south dipping Lapeiquan normal fault was active during the Early Jurassic and latest Early Cretaceous. Early Jurassic extension along the Lapeiquan fault system may have created a half graben in which a coarse-grained sequence of sediments derived from both the Lapeiquan hanging wall and footwall was deposited. The Early Cretaceous phase of extension only occurred along the eastern segment of the Lapeiquan fault that was kinematically linked with the south dipping Qiashikan right-slip normal fault. Both the Early Jurassic and Early Cretaceous extensional events in northern Tibet involve mantle lithosphere as expressed by spatially related basaltic eruptions. The extension is most likely related to back arc processes induced by subduction of the Tethys oceanic plate. The presence of widespread Early Jurassic north-south extension in northern Tibet casts doubts on the early speculation that links Jurassic north-south contraction in the Tian Shan with collisional events along the southern margin of Mesozoic Asia in southern Tibet.

References

Allègre, C. J., et al., Structure and evolution of the Himalayan-Tibet orogenic belt, *Nature*, *307*, 17–22, 1984.

Burchfiel, B. C., Q. Deng, P. Molnar, L. H. Royden, Y. Wang, P. Zhang, and W. Zhang, Intracrustal detachment with zones of continental deformation, *Geology*, *17*, 748–752, 1989.

Burtman, V. S., and P. Molnar, Geological and geophysical evidence for deep subduction of continental crust beneath the Pamir, *Spec. Pap. Geol. Soc. Am.*, *281*, 1–76, 1993.

Chang, C. F., and S. L. Zheng, Tectonic features of the Mount Jolmo Lungma region in southern Tibet, China, *Sci. Geol. Sin.*, *1*, 1–12, 1973.

Che, Z. C., and Y. Sun, The age of the Altun granulite facies complex and the basement of the Tarim basin, *Reg. Geol. China.*, *1*, 51–57, 1996.

Che, Z. C., L. Liu, and Y. Shun, U-Pb, Sm, Rb-Sr, Ar. Ar and $^{18}O/^{16}O$ isotopic studies for early evolution of the structural belt in Altun area, *Acta Geosci. Sin.*, *14*, 334–337, 1995a.

Che, Z. C., L. Liu, H. F. Liu, and J. H. Luo, High-pressure pelitic metamorphic rocks and their geologic setting, *Chin. Sci. Bull.*, *40*, 1298–1300, 1995b.

Cheng, J., and G. Xu, Unpublished geologic map of the Gaize region at a scale of 1:1,000,000 and the geo-

**8 - ** 21

logic report (in Chinese), 369 pp., Xiazang Bur. of Geol. and Miner. Resour., 1986.

Chinese State Bureau of Seismology (CSBS), *The Altyn Tagh Active Fault System*, Seismology Publ. House, Beijing, 1992.

Cowgill, E. S., Tectonic evolution of the Altyn Tagh-Western Kunlun fault system, western China, Ph.D thesis, Univ. of Calif., Los Angeles, 311 pp., 2001.

Cowgill, E., A. Yin, X. F. Wang, and Q. Zhang, Late Cenozoic left-reverse slip movement along the Northern Altyn Tagh Fault and its possible development as the northern boundary of a transpressional strike-slip duplex, *Geology*, 28, 255–258, 2000.

Darby, B. J., G. A. Davis, and Y. Zheng, Structural evolution of the southeastern Daqing Shan, Yinshan belt, Inner Mongolia, China, in *Paleozoic and Mesozoic Tectonic Evolution of Central Asia: From Continental Assembly to Intracontinental Deformation*, edited by M. S. Hendrix and G. A. Davis, *Mem. Geol. Soc. Am.*, 194, 199–214, 2001.

Davis, G. A., X. L. Qian, Y. Zheng, H. Yu, C. Wang, C. Tong, G. E. Gehrels, M. Shafiquallah, and J. E. Fryxell, Mesozoic deformation and plutonism in the Yunmeng Shan: A metamorphic core complex north of Beijing, China, in *The Tectonic Evolution of Asia*, edited by A. Yin and T. M. Harrison, pp. 253–280, Cambridge Univ. Press, New York, 1996.

Davis, G. A., C. Wang, Y. Zheng, J. Zhang, and G. E. Gehrels, The enigmatic Yinshan fold-and-thrust belt of northern China: New views on its intraplate contractional styles, *Geology*, 26, 43–46, 1998.

Davis, G. A., Y. Zheng, C. Wang, B. J. Darby, C. Zhang, and G. Gehrels, Mesozoic tectonic evolution of the Yanshan fold and thrust belt, with emphasis on Hebei and Liaoning provinces, northern China, in *Paleozoic and Mesozoic Tectonic Evolution of Central Asia: From Continental Assembly to Intracontinental Deformation*, edited by M. S. Hendrix and G. A. Davis, *Mem. Geol. Soc. Am.*, 194, 171–197, 2001a.

Davis, G. A., Y. Zhang, C. Zhang, and B. Xu, The Mesozoic Fenging-Longhua and Jiaoqier fault zones, north China: New interpretations of controversial structures, *Geol. Soc. Am. Abstr. Programs*, 33(3), 49, 2001b.

Dewey, J. F., R. M. Shackelton, C. Chang, and Y. Sun, The tectonic evolution of the Tibetan Plateau, *Philos. Trans. R. Soc. London, Ser. A*, 327, 379–413, 1988.

Gehrels, G. E., A. Yin, and X. F. Wang, Detrital-zircon geochronology of the northwestern Tibetan plateau, *Geol. Soc. Am. Bull.*, 115, 881–896, 2003.

Graham, S. A., M. S. Hendrix, C. L. Johnson, D. Badamagarav, J. Amory, M. Porter, R. Barsbold, L. E. Webb, and B. R. Hacker, Sedimentary record and tectonic implications of Mesozoic rifting in southeast Mongolia, *Geol. Soc. Am. Bull.*, 113, 1560–1579, 2001.

Guo, Z. J., Z. C. Zhang, and J. J. Wang, Sm-Nd isochron age of ophiolite along northern margin of Altun Tagh Mountain and its tectonic significance, *Chin. Sci. Bull.*, 44, 456–458, 1999.

Guo, Z. J., Z. C. Zhang, C. Z. Jia, and G. Q. Wei, Tectonics of Precambrian basement of the Tarim craton, *Sc. China Ser.*, 44, 229–236, 2001.

Harrison, T. M., M. T. Heizler, O. M. Lovera, W. Chen, and M. Grove, Chlorine disinfectant for excess argon released from K-feldspar during step heating, *Earth Planet. Sci. Lett.*, 23, 95–104, 1994.

Hendrix, M. S., S. A. Graham, A. R. Carroll, S. R. Sobel, C. L. McKnight, B. J. Schulein, and Z. Wang, Sedimentary record and climatic implications of recurrent deformation in the Tian Shan: Evidence from Mesozoic strata of north Tarim, south Junggar, and Turpan basins, northwest China, *Geol. Soc. Am. Bull.*, 104, 53–79, 1992.

Horton, B. K., A. Yin, M. S. Spurlin, J. Y. Zhou, and J. H. Wang, Paleocene-Eocene syncontractional sedimentation in narrow, lacustrine-dominated basins of east-central Tibet, *Geol. Soc. Am. Bull.*, 114, 771–786, 2002.

Hsü, K., et al., Tectonic evolution of the Tibetan Plateau: A working hypothesis based on the archipelago model of orogenesis, *Int. Geol. Rev.*, 37, 473–508, 1995.

Huo, Y. L., and S. D. Tan, Exploration case history and petroleum geology in Jiuquan continental basin, 211 pp., Pet. Ind. Press, Beijing, 1995.

Jia, C. Z., Tectonic characteristics and petroleum, Tarim Basin, 295 pp., China, Pet. Ind. Press, Beijing, 1997.

Kapp, P. A., A. Yin, C. Manning, M. A. Murphy, T. M. Harrison, L. Din, X. G. Deng, and C. M. Wu, Blueschist-bearing metamorphic core complexes in the Qiangtang block reveal deep crustal structure of northern Tibet, *Geology*, 28, 19–22, 2000.

Kong, A., A. Yin, and T. M. Harrison, Evaluating the role of pre-existing weakness and topography in he Indo-Asian collision using a thin-shell finite element model, *Geology*, 25, 527–530, 1997.

Lin, W., M. Faure, P. Monié, U. Schärer, L. Zhang, and Y. Sun, Tectonics of SE China: New insights from the Lushan massif (Jiangxi Province), *Tectonics*, 19, 852–871, 2000.

Liu, L., Z. C. Che, J. H. Luo, Y. Wang, and Z. I. Gao, Recognition and implication of ecologite in the western Altun Mountains, Xinjiang, *Chin. Sci. Bull.*, 42, 931–934, 1997.

Liu, L., Z. C. Che, Y. Wang, J. H. Luo, and D. L. Chen, The petrological characters and geotetonic setting of high-pressure metamorphic rock belts in Altun Mountains, *Acta Petrol. Sin.*, 15, 57–64, 1999.

Liu, Z. Q., Geologic Map of the Qinghai-Xiang Plateau and its neighboring regions (scale at 1:1,500,000), Chengdu Inst. of Geol. and Miner. Resour., Geol. Publ. House, Beijing, 1988.

Lovera, O. M., F. M. Richter, and T. M. Harrison, The $^{40}Ar/^{39}Ar$ thermochronometry for slowly cooled samples having a distribution of diffusion domain sizes, *J. Geophys. Res.*, 94, 17,917–17,935, 1989.

Lovera, O. M., M. Grove, T. M. Harrison, and K. I. Mahon, Systematic analysis of K-feldspar $^{40}Ar/^{39}Ar$ step-heating experiments I: Significance of activation energy determinations, *Geochim. Cosmochim. Acta*, 61, 3171–3192, 1997.

Lovera, O. M., M. Grove, and T. M. Harrison, Systematic analysis of K-feldspar $^{40}Ar/^{39}Ar$ step-heating experiments II: Relevance of laboratory K-feldspar argon diffusion properties to Nature, *Geochim. Cosmochim. Acta*, 66, 1237–1255, 2002.

Murphy, M. A., A. Yin, T. M. Harrison, S. B. Durr, Z. Chen, F. J. Ryerson, K. S. F. Kidd, X. F. Wang, and X. Zhou, Significant crustal shortening in southern Tibet prior to the Indo-Asian collision, *Geology*, 25, 719–722, 1997.

Paces, J. B., and J. D. Miller, Precise U-Pb age of Duluth Complex and related mafic intrusions, northeastern Minnesota: Geochronological insights into physical, petrogenetic, paleomagnetic, and tectonomagmatic processes associated with the 1.1 Ga midcontinent rift system, *J. Geophys. Res.*, 98, 13,997–14,013, 1993.

Peltzer, G., and P. Tapponnier, Formation and evolution of strike-slip faults, rifts, and basins during the India-Asia collision: An experimental approach, *J. Geophys. Res.*, 93, 15,085–15,117, 1988.

Ratschbacher, L., B. R. Hacker, L. E. Webb, M. McWilliams, T. Ireland, S. Dong, A. Calvert, D. Chateigner, and H. R. Wenk, Exhumation of the ultrahigh-pressure continental crust in east central China: Cretaceous and Cenozoic unroofing and the Tan-Lu fault, *J. Geophys. Res.*, 105, 13,303–13,338, 2000.

Ren, J. Y., K. Tamaki, S. T. Li, and Z. Junxia, Late Mesozoic and Cenozoic rifting and its dynamic setting in Eastern China and adjacent areas, *Tectonophysics*, 344, 175–205, 2002.

Ritts, B. D., and U. Biffi, Magnitude of post-Middle Jurassic Baojocian displacement on the central Altyn Tagh fault system, northwest China, *Geol. Soc. Am. Bull.*, 112, 61–74, 2000.

Rumelhart, P., A. Yin, R. Butler, E. Cowgill, Q. Zhang, and X. Wang, Cenozoic vertical-axis rotation of southern Tiarim: Constraints on the tectonic evolution of the Altyn Tagh fault system, *Geology*, 27, 819–822, 1999.

Shen, Z.-K., M. Wang, Y. Li, D. D. Jackson, A. Yin, D. Dong, and P. Fang, Crustal deformation along the Altyn Tagh fault system, western China, from GPS, *J. Geophys. Res.*, 106, 30,607–30,621, 2001.

Sobel, E. R., Basin analysis of the Jurassic-Lower Cretaceous southwest Tarim basin, NW China, *Geol. Soc. Am. Bull.*, 111, 709–724, 1999.

Sobel, E. R., and N. Arnoad, A possible middle Paleozoic suture in the Altyn Tagh, NW China, *Tectonics*, 18, 64–74, 1999.

Sobel, E. R., N. Arnaud, M. Jolivet, B. D. Ritts, and M. Brunel, Jurassic to Cenozoic exhumation history of the Altyn Tagh range, NW China constrained by $^{40}Ar/^{39}Ar$ and apatite fission track thermochronolology, *Mem. Geol. Soc. Am.*, 194, 247–267, 1996.

Vincent, S. J., and M. B. Allen, Evolution of the Minle and Chaoshui Basins, China: Implications for Mesozoic strike-slip basin formation in Central Asia, *Geol. Soc. Am. Bull.*, 111, 725–742, 1999.

Webb, L. E., S. A. Graham, C. L. Johnson, G. Badarch, and M. S. Hendrix, Occurrence, age, and implications of the Yagan Onch Hayrhan metamorphic core complex, southern Mongolia, *Geology*, 27, 143–146, 1999.

Xinjiang Bureau of Geology and Mineral Resources (BGMR), Geologic map of the Bashikaogong sheet at a scale of 1:200,000, Chin. Minist. of Geol. and Miner. Resour., Beijing, 1981a.

Xinjiang Bureau of Geology and Mineral Resources (BGMR), Geologic map of the Lenghu sheet at a scale of 1:200,000, Chin. Minist. of Geol. and Miner. Resour., Beijing, 1981b.

Xinjiang Bureau of Geology and Mineral Resources (BGMR), Geologic map of the Duobagou sheet at a scale of 1:200,000, Chin. Minist. of Geol. and Miner. Resour., Beijing, 1981c.

Xinjiang Bureau of Geology and Mineral Resources (BGMR), Geologic map of the Xorkoli sheet at a scale of 1:200,000, Chin. Minist. of Geol. and Miner. Resour., Beijing, 1981d.

Xinjiang Bureau of Geology and Mineral Resources (BGMR), Geologic map of the E-Bo-Liang sheet at a scale of 1:200,000, Chin. Minist. of Geol. and Miner. Resour., Beijing, 1986.

Xinjiang Bureau of Geology and Mineral Resources (BGMR), *Regional Geology of the Xinjiang Uygur Autonomous Region*, 579 pp., Geol. Publ. House, Beijing, 1993.

Yang, S. J., F. C. Meng, J. X. Zhang, and H. B. Li, The shoshonitic volcanic rocks at Hongliuxia: Pulses of Altyn Tagh fault in Cretaceous?, *Sci. China, Ser. D*, 44, supplement, 94–102, 2001.

Yin, A., and T. M. Harrison, Geologic Evolution of the Himalayan-Tibetan orogen, *Annu. Rev. Earth Planet. Sci.*, 28, 211–280, 2000.

Yin, A., and S. Nie, A Phanerozoic palinspastic reconstruction of China and its neighboring regions, in *The Tectonic Evolution of Asia*, edited by A. Yin and T. M. Harrison, pp. 442–485, Cambridge Univ. Press, New York, 1996.

Yin, A., T. M. Harrison, F. J. Ryerson, W. Chen, W. S. F. Kidd, and P. Copeland, Tertiary structural evolution of the Gangdese thrust system in southern Tibet, *J. Geophys. Res.*, 99, 18,175–18,201, 1994.

Yin, A., G. Gehrels, X. Chen, X. Wang, and T. M. Harrison, Normal-slip motion on the northern Altyn

Tagh fault, *Eos Trans. AGU*, *81*(48), Fall Meet. Suppl., Abstract T52B-08, 2000.

Yin, A., et al., Tectonic history of the Altyn Tagh fault in northern Tibet inferred from Cenozoic sedimentation, *Geol. Soc. Am. Bull.*, *114*, 1257–1295, 2002.

Zhang, J. X., Z. M. Zhang, Z. Q. Xu, J. S. Yang, and J. W. Cui, Petrology and geochronology of eclogites from the western segment of the Altyn Tagh, northwestern China, *Lithos*, *56*, 187–206, 2001.

Zhang, Z., G. Zhaojie, and H. Zuozhen, Geochemistry and geological significance of the mid-Jurassic volcanic rocks in Dunhuang Basin (in Chinese with English abstract), *Acta Sci. Univ. Pekinensis*, *34*, 72–79, 1998.

Zheng, Y. D., and Q. Zhang, The Yangan metamorphic core complex and extensional detachemnt in Inner Monglia, China, *Acta Geol. Sin.*, *7*, 1145–1154, 1994.

Zheng, Y. D., G. A. Davis, and B. J. Darby, A field trip guide for the field conference of Mesozoic extensional tectonics in eastern China and Mongolia, Huhhot, Nei Mongol, 14 pp., Bur. of Geol. and Miner. Resourc., Nei Mongol Autonomous Reg., China, Hohhot, 2001.

Zorin, V. A., Geodynamics of the western part of the Mongolia-Okhotsk collisional belt, Trans-Baikal region (Russia) and Mongolia, *Tectonophysics*, *306*, 33–56, 1999.

―――――――――

X. Chen and X.-F. Wang, Institute of Geomechanics, Chinese Academy of Geological Sciences, Beijing 100081, China.

G. E. Gehrels, Department of Geosciences, University of Arizona, Tucson, AZ 85721, USA.

A. Yin, E. S. Cowgill, M. Grove, and T. M. Harrison, Department of Earth and Space Sciences, University of California, Los Angeles, CA 90095-1567, USA. (yin@ess.ucla.edu)